Core-level binding-energy shifts for the metallic elements

Börje Johansson
Sekt. 214, FOA 2, S-104 50 Stockholm, Sweden

Nils Mårtensson
Institute of Physics, Uppsala University, S-751 21 Uppsala, Sweden
(Received 5 March 1979; revised manuscript received 15 October 1979)

A general treatment of core-level binding-energy shifts in metals relative to the free atom is introduced and applied to all elemental metals in the Periodic Table. The crucial ingredients of the theoretical description are (a) the assumption of a fully screened final state in the metallic case and (b) the $(Z+1)$ approximation for the screening valence charge distribution around the core-ionized site. This core-ionized site is, furthermore, treated as an impurity in an otherwise perfect metal. The combination of the complete screening picture and the $(Z+1)$ approximation makes it possible to introduce a Born-Haber cycle which connects the initial state with the final state of the core-ionization process. From this cycle it becomes evident that the main contributions to the core-level shift are the cohesive energy difference between the $(Z+1)$ and Z metal and an appropriate ionization energy of the $(Z+1)$ atom (usually the first ionization potential). The appearance of the ionization potential in the shift originates from the assumption of a charge-neutral final state, while the contribution from the cohesive energies essentially describes the change of bonding properties between the initial and final state of the site. The calculated shifts show very good agreement with available experimental values (at present, for 19 elements). For the other elements we have made an effort to combine experimental ionization potentials with theoretical calculations in order to obtain accurate estimates of some of the atomic-core-level binding energies. Such energies together with measured metallic binding energies give "pseudoexperimental" shifts for many elements. Our calculated core-level shifts agree exceedingly well also with these data. For some of the transition elements the core-level shift shows a deviating behavior in comparison with that of neighboring elements. This is shown to be due to a difference in the atomic ground-state configuration, such as, for example, d^5s in chromium relative to the d^ns^2 configuration in vanadium and manganese. When the core-level shift is referred to, the d^ns^2 (or $d^{n+1}s$) atomic configuration for all the elements in a transition series, a quite regular behavior of the shift is found. However, some structure can still be observed originating from a change of screening within the d band from a bonding to an antibonding type as one proceeds through the series. For elements beyond the coin metals the screening of a core hole is performed by p electrons, which provide a less effective screening mechanism than the d electrons for the transition metals. The coin metals are intermediate cases, partly due to a dominating s-electron screening and partly due to d-electron bonding in the initial state. The effect of the electron-density redistribution between the free atom and the solid on the core-level shift is particularly striking in the case of the rare-earth elements Pr-Sm and Tb-Tm. Here the remarkable situation is that a deep core electron is less bound in the atom than in the solid. Also for the actinides the electronic redistribution upon condensation gives rise to pronounced effects on the core-level shifts. Further, it is shown that the measured $6p_{3/2}$ binding energy in metallic uranium provides a clear demonstration of the occupation of the $5f$ level in this metal. The present treatment of the core-level shift for bulk metallic atoms can easily be generalized to surface atoms. From an empirical relation for the surface energy a simple expression for the shift of the surface core-level relative to the bulk can be derived. For the earlier transition metals, it is found that the core electrons are more bound at the surface than in the bulk, while for the heavier ones the opposite situation exists. This change of sign of the surface shift depends on the bonding-antibonding division of the d band. To illustrate how the present approach can be applied to alloy systems, a treatment of core-level shifts for rare-gas atoms implanted in noble metals is undertaken.

I. INTRODUCTION

A considerable amount of experimental work during the last two decades has been directed to the study of core-level binding energies.[1-3] It was realized early that these binding energies depend on the chemical environment of the atom. In order to profit fully from the electron-spectroscopic results, it is important that these binding-energy shifts are properly understood. Of special importance is the core-electron binding-energy shift between the free atom and the condensed atom in its metallic state. The significance of this problem is reflected by the large number of recent papers devoted to this subject.[4-21]

Previously there has been a lack of experimental core-electron binding energies for free atoms. Therefore, in the theoretical work, which has been mainly focused on the $3d$ elements, it has become common to compare theory with so called "quasiexperimental" data, where theoretical estimates of atomic binding energies are used

together with measured core levels for the solids. However, recent experimental efforts in the study of free atoms give promise that this unsatisfactory situation will become somewhat remedied in the near future. In fact, for most of the nontransition metals there already exist experimentally determined atomic binding energies. These have been obtained in a variety of ways. Some have been measured directly in photoionization experiments (e.g., Refs. 19–25). A lot of the data have been collected from photoabsorption measurements (e.g., Refs. 26–34). Binding energies have also been derived from Auger electron spectroscopy, where either electron[35-39] or fast ion-beam collision excitation has been used.[40-42] Some of these new data will be incorporated in the present paper.

For the free atoms the experimental binding energies are referenced to the vacuum zero. In the metallic state the core-electron binding energies are measured relative to the Fermi level E_F. Therefore, it is a definite advantage if a theory can be developed that gives a direct connection between these two *measured* quantities. Thereby, the difficulty as to what sample work function to use can be avoided. In the present paper a theory with this practical merit will be presented. This theory also lends itself to simple generalizations so that, for example, surface effects on the core-level binding energies can be treated. Similarly, rare gases implanted in noble-metal hosts can also be considered. In a more general context this paves the way towards a treatment of core-level shifts in alloys and intermetallic compounds.

The paper is organized as follows: In Sec. II we introduce a thermodynamical cycle which describes the core-electron excitation process. The essential ingredients are the complete screening concept and the $(Z+1)$ approximation. In Sec. III we compare theory with experiment for nontransition elements. In the three following sections, IV–VI, the $3d$, $4d$, and $5d$ transition series are considered, respectively. Core-level shifts for the $4f$ and $5f$ elements are treated in Sec. VII. That the $6p$-level binding energy in uranium metal provides important information concerning the $5f$ occupancy is demonstrated in Sec. VIII. The core-level binding-energy shift between bulk and surface atoms is treated in Sec. IX. Rare gases implanted in the noble metals are discussed in Sec. X. Section XI contains a summary and discussion of the results. Finally, semiempirical core-level binding energies are calculated for a number of elements in the Appendix. A short account of the present work will be published elsewhere.[43]

II. THEORETICAL MODEL

The core-level binding-energy shift δE_c is given by the difference of two binding energies,

$$\delta E_c = [E^A(n_c-1) - E^A(n_c)] - [E^M(n_c-1) - E^M(n_c)] = E_c^A - E_c^M , \quad (1)$$

where $E(n_c)$ is the total binding energy of the system with n_c electrons in the core level labeled c. The superscripts A and M refer to the atomic and metallic case, respectively. E_c^A is the binding energy of the core level c for the atom and E_c^M the corresponding quantity for the metal. In Eq. (1) both binding energies are referred to the vacuum level. However, experimentally, the core-level binding energies for the metal are measured relative to the Fermi level, while for the free atoms the vacuum zero is the reference level. Therefore, one has to add the metallic work function ϕ to the experimental metallic core-level binding energy in order to bring the two binding energies to a common energy scale. However, the experimental determination of the work function is most difficult and impaired by a rather large uncertainty.[44(a)] In the present paper we will avoid this difficulty and derive a direct and simple relation between the atomic binding energy, E_c^A, and the binding energy in the metallic state of the atom relative to the Fermi energy, $E_{c,F}^M$. Thus the energy shift ΔE_c which we will discuss for the most part of this work is given by

$$\Delta E_c = E_c^A - E_{c,F}^M . \quad (2)$$

The relation between ΔE_c and the previous δE_c in Eq. (1) is[44(b)]

$$\delta E_c = \Delta E_c - \phi . \quad (3)$$

In earlier treatments it is the δE_c shift which has received attention. Relation (3) can be used to give a connection between our present work and the previous theoretical work. However, we stress once more that the advantage of using ΔE_c is that the energies involved can both be determined with a high experimental accuracy.

The picture we will apply to the core-ionization process in the metal is the following one: First, we consider the ionization as taking place at a particular atomic site in the solid. Second, we assume that the site from which the core electron is ejected will become totally screened by the surrounding conduction electrons.[45,46] Thus the final state will be considered as an "impurity" in an otherwise perfect crystal. Since the binding energy is referred to the Fermi level, this means that $E_{c,F}^M$ can be regarded as the excitation energy of the core electron to the Fermi level.[47] Thus the initial state is the perfect metal and the final

state is a core-hole impurity site (completely screened) in an otherwise perfect crystal.

However, it turns out that this final state can be reached from the original perfect metallic state by means of a Born-Haber process. This is illustrated in Fig. 1. First we remove one atom from the metal Z and arrive at the free atom, a process which defines the cohesive energy $E_{\rm coh}^{Z}$. Ionization of the core electron of the free atom involves the energy E_c^A. (For the sake of the argument we will assume an infinite lifetime of the created core hole). This Z^* ion (with a hole in the core level c) is neutralized by the acquisition of an electron into the lowest valence shell state of the Z^* atom (in presence of the core hole), thereby releasing the "ionization" energy I^{Z^*}. After this, we bring together a macroscopic number of such prepared Z^* atoms to form a solid, yielding the cohesive energy $E_{\rm coh}^{Z^*}$. One of these metallic sites is then dissolved in the host metal Z. The energy involved in this last step is the solution energy (for the infinitely dilute case) of the Z^* metal in the Z metal, $E_{Z^*}^{\rm imp}(Z)$. Thus any charge transfer is included in this term.

The completed cycle obeys the following relation:

$$E_{c,F}^{M} = E_{\rm coh}^{Z} + E_c^A - I^{Z^*} - E_{\rm coh}^{Z^*} + E_{Z^*}^{\rm imp}(Z)\,, \tag{4}$$

and the desired energy shift ΔE_c is simply given by

$$\Delta E_c = E_c^A - E_{c,F}^{M} = I^{Z^*} + E_{\rm coh}^{Z^*} - E_{\rm coh}^{Z} - E_{Z^*}^{\rm imp}(Z)\,. \tag{5}$$

Equation (4) is the exact expression of the *thermal* (adiabatic) excitation of the core electron c from an atom at a specific site to the Fermi level. However, photoexcitation is a vertical process and therefore Eq. (4) will in principle be a lower limit to the actual experimental value. However, as will be briefly discussed later, this distinction can in many cases be disregarded.

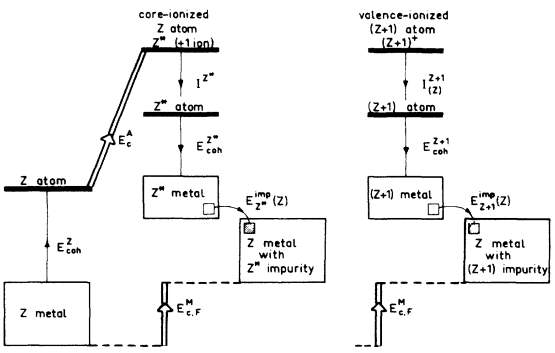

FIG. 1. The Born-Haber cycle for calculation of the $E_{c,F}^{M}$ excitation energy. Its construction is described in the text. The $(Z+1)$ approximation is shown to the far right.

Even if the quantity $E_{\rm coh}^{Z}$ is available from thermochemical data, this is certainly not the case for the other quantities in Eq. (5). Therefore, it might seem that our transcription of the excitation process into a Born-Haber cycle provides no particular advantage. However, examining in Fig. 1 the steps leading from the core-ionized atom to the core-hole impurity site, we note that it is the acquisition of a *valence* electron and the redistribution of the total *valence* electron charge in the metallic environment which comes into play. Thus, it is the valence-electron density distribution which determines the energies I_{Z^*}, $E_{\rm coh}^{Z^*}$, and $E_{Z^*}^{\rm imp}(Z)$. However, as regards the atomic valence-electron orbitals, a core with one electron removed from a deep-lying inner shell can be replaced quite accurately by the core of the $(Z+1)$ atom. Similarly, as far as the conduction electron structure is involved, the final state resulting from the photoejection of a core electron can be described by an almost equivalent one, namely, by a $(Z+1)$ atomic site in the original Z metal. This means that the right-hand part of the Born-Haber cycle in Fig. 1 may be replaced by an almost equivalent one as illustrated to the far right in Fig. 1. Thus the core-ionized atomic state is replaced by a valence-ionized $(Z+1)$ atom with the same valence structure as the core-ionized Z atom. This $(Z+1)$ ion with a valence-shell vacancy is neutralized by the acquisition of an electron forming the atomic ground state of the neutral $(Z+1)$ atom. This process involves the ionization energy $I_{(Z)}^{Z+1}$. The remaining steps leading to the $(Z+1)$ impurity in the Z metal in Fig. 1 are self-explanatory. The use of the $(Z+1)$ approximation thus leads to the following approximate expression for $E_{c,F}^{M}$:

$$E_{c,F}^{M} = E_{\rm coh}^{Z} + E_c^A - I_{(Z)}^{Z+1} - E_{\rm coh}^{Z+1} + E_{Z+1}^{\rm imp}(Z)\,, \tag{6}$$

and, accordingly the binding energy shift ΔE_c is given by

$$\Delta E_c = I_{(Z)}^{Z+1} + E_{\rm coh}^{Z+1} - E_{\rm coh}^{Z} - E_{Z+1}^{\rm imp}(Z)\,. \tag{7}$$

For a metal in the middle of the $3d$, $4d$, or $5d$ transition series, the atomic volume does not change very much upon replacement of a Z atom by a $(Z+1)$ atom, so, in this case the difference between the vertical and thermal excitation energies will be almost negligible. On the other hand, in the case of the alkali metals this difference may be of significance since here the atomic volumes of the Z and $(Z+1)$ atom differ appreciably. However, since we will in any case obtain $E_{Z+1}^{\rm imp}(Z)$ from an approximate treatment (see below) and since the dominating contributions to ΔE_c in Eq. (7) come from the other terms, we will not, in the following, make any distinction between

the vertical and thermal excitations. The solution energy of the $(Z+1)$ impurity in the Z metal, $E^{\rm imp}_{Z+1}(Z)$, could in principle be obtained from thermochemical measurements. However, such data are somewhat sparse and we have instead chosen to use Miedema's semiempirical scheme[48] for deriving relatively appropriate values for the $E^{\rm imp}$ term.

As is obvious from the description above, the present picture of the core-level binding-energy shift does not depend on which particular inner shell (c) is ionized. This is due to the fact that the $(Z+1)$ approximation, as applied here, does not make any discrimination between the core levels. In the very few cases where sufficient experimental data are available both for the free atom and the metal, this is found to be a good approximation.[49] As concerns the absolute error of the $(Z+1)$ approximation to the ionization energy, I^{Z*}, we have, for some specific cases, observed that it does not introduce an error beyond 0.2 eV.[51] In a future communication this aspect will be more thoroughly investigated.[54] A relatively mild dependence on the core level c may, in general, be anticipated.

It is likely that the $(Z+1)$ approximation, $E^{Z+1}_{\rm coh}$, to the cohesive energy $E^{Z*}_{\rm coh}$, does not introduce any appreciable error. This view is supported by the cohesive energies of the rare-earth elements. Here the appropriate cohesive energy function is practically identical (within the experimental errors) for all the lanthanides,[55] despite the fact that in this series we compare cohesive energies for elements having everything from no core hole in the f^{14} configuration (i.e., lutetium), up to having 14 core holes in the f shell (i.e., lanthanum). Instead, from the regular behavior of the cohesive energy in the Periodic Table,[56,57] it seems that it is the number of valence electrons and their (s,p,d) character that largely determine the cohesive energies. In view of this expected accuracy of the $(Z+1)$ approximation for the cohesive energy, the $(Z+1)$ approximation for the $E^{\rm imp}_{Z*}(Z)$ term should be correspondingly accurate. In the following four sections we will compare calculated core-level shifts ΔE_c, Eq. (7), with presently available experimental data. The cohesive energies are taken from the tabulation by Brewer[57] and the ionization potentials and optical data are from Refs. 58–61.

III. CORE-LEVEL SHIFTS FOR SIMPLE METALS

For most metals in the Periodic Table at least some of the core-level binding energies have been quite accurately determined. In contrast to this, experimental data for the free atoms are much more limited. Currently, there are free-atom data available for many of the simple metals, the alkaline earths as well as copper and silver. In Fig. 2 we compare for these elements the experimental binding-energy shifts between the atom and the metal[62] with the values derived from Eq. (7). As can be seen, the agreement is generally very good. However, it is also evident from the figure that for most of the elements there is a considerable scatter in the experimental values. There might be a variety of reasons for this as, for instance, insufficient calibration.[73]

Regarding the calculated values, the largest uncertainty is probably introduced by the $E^{\rm imp}_{Z+1}(Z)$ term. For instance, for the alkali metals the Miedema values are quite large and positive (~0.5 eV) and might quite well be impaired by a rather large error. Further, as already mentioned, the difference for these metals between the thermal and vertical excitations may also be of some importance.

In view of the successful correlation between the calculated and the measured binding-energy shifts, it seems clear that the present picture of the metallic core-electron ionization indeed incorporate the most important features. Equally accurate results have previously been obtained for the lanthanides.[76] Therefore, one would expect that the present approach will be applicable to all metals in the Periodic Table.

IV. 3d TRANSITION ELEMENTS

In this section we will compare the theoretical values derived from Eq. (7) with experimental and "pseudo experimental" binding-energy shifts for the metallic elements in the fourth period of the Periodic Table (K–Ga). In addition to the elements already treated in Sec. III. (K, Ca, Cu, and Zn), there are also experimental data available[32] for Mn, Co, Fe, and Ni. However, in these latter cases the data are from $3p$ photoabsorption measurements made in the vapor and solid phases. It is known that these spectra in general appear much the same in the two phases. In some cases there is, however, a clear shift in the threshold energy spectra. These shifts can now be treated in the same way as the core holes[77] in Fig. 1. The only difference is that there is no longer any neutralization step involving $I^{Z+1}_{(Z)}$. The shift of the measured absorption edge, Δ_a, will therefore obey the relation

$$\Delta_a = E^{Z+1}_{\rm coh} - E^{Z}_{\rm coh} - E^{\rm imp}_{Z+1}(Z)\,. \tag{8}$$

In order to treat these data on the same energy scale as the other elements (like in Fig. 2), we

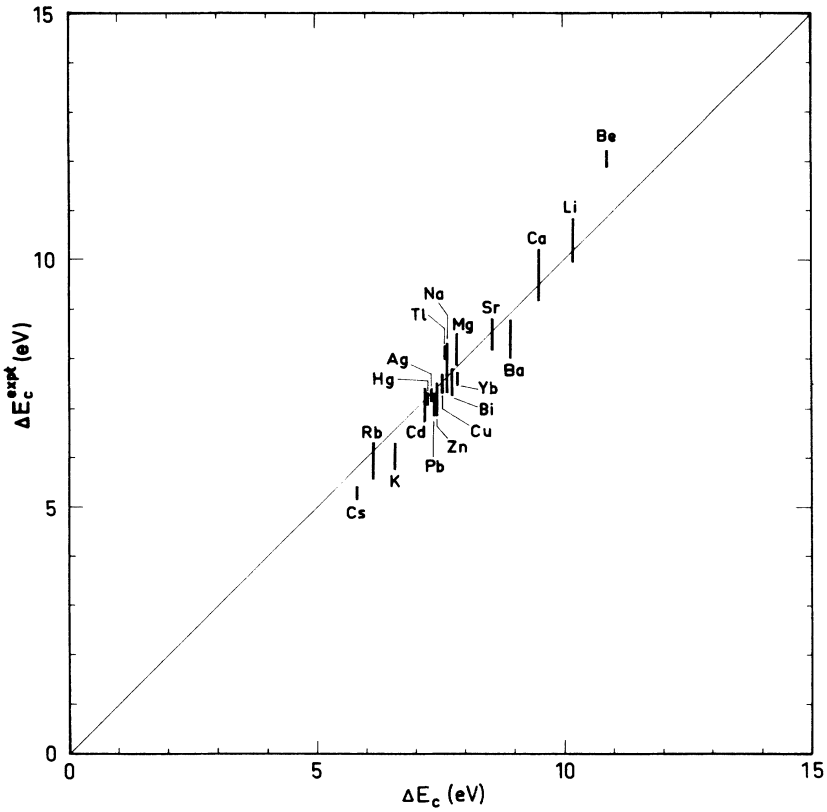

FIG. 2. Comparison between the experimental and theoretical core-level binding-energy shifts; ΔE_c^{expt} (vertical axis) and ΔE_c (horizontal axis), respectively. The height of the bars does not correspond to the experimental error, but rather the spread of data from different experiments. The somewhat deviating value for Be will be explained in a future communication (Ref. 54).

just add $I_{(Z)}^{Z+1}$ to the experimental absorption shift.

For the remaining elements (Sc, Ti, V, Cr, and Ga) there are no data available for the free atoms. However, here we have calculated $3p$ (Sc–Cr) and $3d$ (Ga) core-electron ionization energies by means of an indirect method described in the Appendix. The procedure leans heavily on spectroscopic data, and some test examples show that the derived ionization energies should be quite accurate. The calculated atomic binding energies combined with measured energies for the metal[78] gives "pseudoexperimental" data for the core-level binding-energy shifts. The mentioned experimental and "pseudoexperimental" data are compared with the calculated values in Fig. 3. The agreement is good.

In comparison with earlier theoretical work on core-level shifts, the present approach shows a considerably improved agreement with experiment. The claimed uniform level of agreement for the $2s$ level binding-energy shift for the $3d$ elements in Ref. 7 is based on a comparison with quasiexperimental data, where calculated atomic binding energies[79] are used in combination with experimental metallic binding energies.[9] However, recent experimental work has shown that these calculated atomic binding energies are rather inaccurate. The atomic Dirac-Slater calculations in Ref. 79 are only performed for $Z \leq 29$. However, for these elements the results are almost identical (except for chromium[80]), to the more recent Dirac-Slater results in Ref. 81 which cover the whole periodic system. Using the results from these latter calculations we can observe that the calculated value for the $2s$ binding energy is 1933.4 eV for Kr, while the experimental value[1] is 1924.6(8) eV, i.e., a difference of about 9 eV. Similarly, for Zn an experimental value[82] of 1203.2 eV can be derived, which should be compared with a calculated value of 1207.5 eV. Again, a considerable deviation. In addition to these difficulties it should also be mentioned that the experimental metallic $2s$ binding energies sometimes show a considerable scatter from one investigation to another.

As already pointed out in Ref. 6, the deviating value for Cr in Fig. 3 is due to the fact that the Cr atom has a $d^{m-1}s$ atomic configuration rather

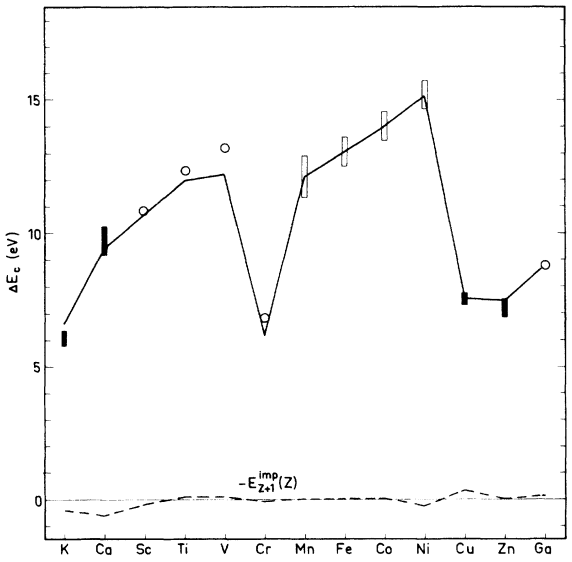

FIG. 3. The full line is the calculated core-level binding-energy shift, Eq. (7), for the metallic elements of the fourth period. The experimental data denoted by dark bars are discussed in Ref. 62. For the experimental data denoted by white bars see the discussion in the text in connection with Eq. (8). The open circles correspond to "pseudoexperimental" data derived from calculated atomic ionization energies (Method A in the Appendix) and experimental metallic binding energies. The dotted line is the impurity contribution to the shift.

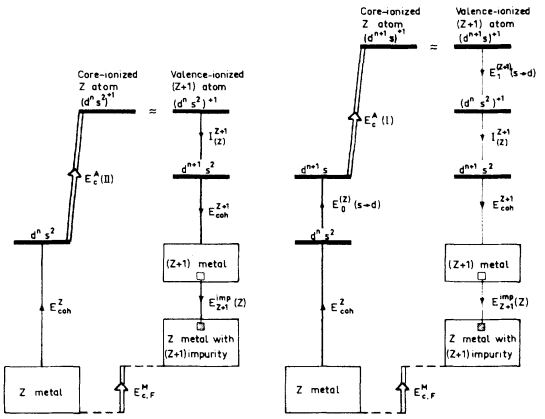

FIG. 4. Comparison between the "divalent" ΔE_c^{II} and "monovalent" ΔE_c^{I} level shifts for the $3d$ elements, where $\Delta E_c^{II} = E_c^A(II) - E_{c,F}^M$ and $\Delta E_c^{I} = E_c^A(I) - E_{c,F}^M$. The quantities $E_c^A(II)$ and $E_c^A(I)$ are the atomic binding energies for the divalent and monovalent configuration, respectively. The figure to the left illustrates the divalent shift and the one to the right shows the monovalent shift. Note that the only difference between these two Born-Haber cycles is to be found in the two excitation energies of the form $d^n s^2 \rightarrow d^{n+1}s$ [$E_0^{(Z)}(s \rightarrow d)$ for the Z atom and $E_1^{(Z+1)}(s \rightarrow d)$ for the $(+1)$ ion of the $(Z+1)$ element]. Thus the difference between the divalent and monovalent shift can be obtained directly from these two spectroscopic energies.

than the $d^n s^2$ configuration which prevails for the other $3d$ atoms. The same explanation was also given for the drop between Ni and Cu, which seems most reasonable in view of the $d^{n+1}s$ atomic configuration in Cu. However, the authors of Ref. 4 ascribed this drop to an s-electron final-state screening in Cu in contrast to the d-electron screening for the other $3d$ elements. Below, we will show that the true reason for the drop between Ni and Cu is indeed a combination of both these circumstances.

In the case where the atomic configuration is $d^{n+1}s$, we will refer to this as being of a "monovalent" type. Similarly, when the atomic configuration is $d^n s^2$, this will be referred to as "divalent".[84] Within the present formulation it is easy to calculate the ΔE_c^{I} shifts for the case that all the $3d$ elements were monovalent as free atoms. The same is true for the ΔE_c^{II} shifts, where all the $3d$ elements are assumed to have a divalent atomic configuration. This is illustrated in Fig. 4. As can be seen from this figure, certain atomic-spectroscopic energies have to be added to Eq. (7) in order to make this relation appropriate for the monovalent (or divalent) case. The obtained ΔE_c^{I} and ΔE_c^{II} shifts are displayed in Fig. 5. Both ΔE_c^{I} and Δ_c^{II} behave in a relatively smooth way through the series. Furthermore, both of them show a dip between Ni and Cu, which clearly demonstrates a different final-state screening mechanism in copper as compared to the other $3d$ elements. However, this dip is not as pronounced as the difference between the monovalent and divalent ΔE_c shifts. Thus the

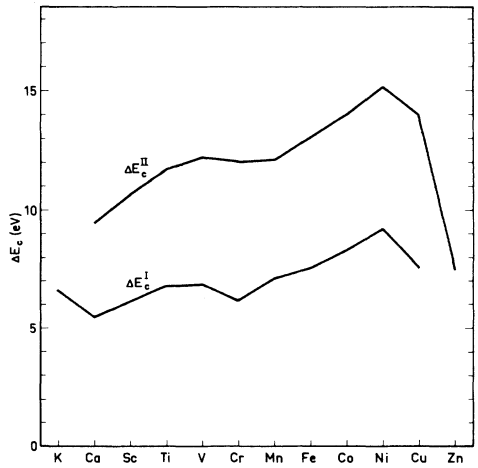

FIG. 5. Comparison between calculated values for the monovalent shift, ΔE_c^{I}, and the divalent shift, ΔE_c^{II}. These quantities are illustrated and described in connection with Fig. 4.

main reason for the large drop between Ni and Cu in Fig. 3 is due to the monovalent atomic property of Cu. However, the somewhat different screening mechanism in Cu gives an enhancement of the drop in the energy shift between Ni and Cu.

From Fig. 5 we also note a pronounced difference in ΔE_c^{II} between Cu and Zn. This is mainly due to the fact that the screening charge in Zn is predominantly of p character, while in Cu the screening associated with the ΔE_c^{II} shift is a combination of d and s screening. Since the p orbital is spatially more extended than the d and s orbitals, this means that the final-state screening in Zn is not as effective as in Cu. On the other hand, the ΔE_c shift is similar for Cu and Zn (i.e., ΔE_c^{I} for Cu and ΔE_c^{II} for Zn), Fig. 3. Thus, in this comparison the mentioned difference in the final-state screening is outweighted by an initial state effect, namely, the participation of the d electrons in the bonding of Cu but not in Zn. When comparing the ΔE_c shifts between Zn and Ga, we find that they are rather similar to each other. The reason for this is that in both cases the screening charge is of p type.

The use of Eq. (7) in the calculation of the ΔE_c value for Ga needs special mention. The $(Z+1)$ approximation here involves the element Ge. As an impurity in Ga, the "Ge" atomic site should be considered to be in its metallic phase. Therefore, the quantity E_{coh}^{Z+1} should not be the experimental cohesive energy for germanium, but should rather correspond to the cohesive energy for the hypothetical metallic phase of germanium. Further, the Miedema parameters for germanium also refer to this metallic phase. The metallic cohesive energy of germanium has been estimated[48] to be 3.6 eV.

Finally, we note from Fig. 5 that both ΔE_c^{II} and ΔE_c^{I} show kind of a plateau region in the middle of the series. This is because for the earlier transition elements, the final-state screening takes place in the bonding part of the d band, while for the heavier elements antibonding d states are utilized. This will be further discussed in Sec. IX in connection with surface core-level shifts. Suffice it here to say that the inflection point in ΔE_c^{II} and ΔE_c^{I} occurs for chromium, indicating that this element is close to having a half-filled d band.

V. 4d TRANSITION ELEMENTS

For the metallic elements of the fifth period there are much less experimental data available than for the 3d elements. It is only in the beginning (Rb, Sr) and in the latter part of the series (Ag, Cd) that experimental values[62] for the core-level binding-energy shifts can be found. For Y and Zr we have for the $4p_{3/2}$ level derived "pseudoexperimental" atomic values of the same type as in the earlier elements of the 3d transition series (see Appendix). Unfortunately, due to lack of spectroscopic information, this method can not be used for elements beyond Zr, except for a few cases in the heavier part of the fifth period where the $4d_{5/2}$ level is derived (In, Sn). Instead, we have used a somewhat different method from which we calculate the atomic binding energies of the $3d_{5/2}$ core levels throughout the whole series. Since this method is a kind of an interpolation procedure, based on experimental data for Zn, Kr, Sr, Cd, and Xe, the calculated values should be quite reliable. The details of these calculations are deferred to the Appendix. In Fig. 6 we compare the experimental[62] and "pseudoexperimental"[85] shifts with our theoretical values. The agreement is satisfactory. The reason that no pseudoexperimental point has been included for Tc is that currently there are no accurate experimental binding energies available for the Tc metal. However, the good agreement obtained in Fig. 6 indicates that we can combine our interpolated $3d_{5/2}$ binding energy with our calculated shift to derive a fairly accurate binding energy for the solid phase. The obtained value is 254.4 eV. This can be compared with the previously reported value[2] of 253 eV. Inspection of Fig. 6 shows that the error in the estimated Tc binding energy should not exceed 0.5 eV.

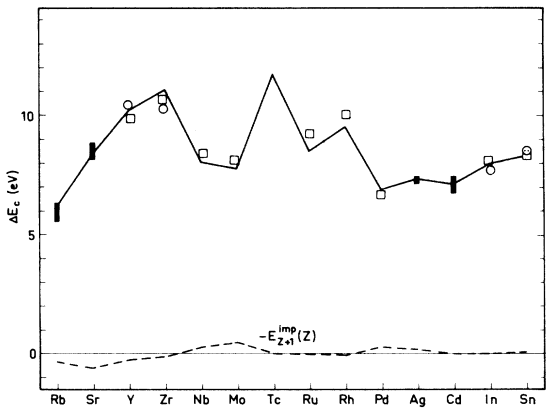

FIG. 6. The full line is the calculated core-level binding-energy shift, Eq. (7), for the metallic elements in the fifth period. The experimental and pseudoexperimental data have the same notation as in Fig. 3. The open circles refer to the $4p_{3/2}$ (Y, Zr) and $4d_{5/2}$ shifts (In, Sn). In addition, the open squares refer to pseudoexperimental values for the $3d_{5/2}$ level obtained from Method B in the Appendix. The dotted line is the impurity contribution to the shift.

Among the 4*d* elements, we find in many cases dips in the ΔE_c values (Fig. 6). In the cases of Nb, Mo, Ru, and Rh, this is due to the monovalent, $d^{m+1}s$, atomic ground-state configuration. For Pd there is an additional dip in comparison with Ru and Rh. This is explained by its "zero-valent" atomic ground-state configuration, d^{10}. Otherwise, the characteristic features found in the 3*d* transition elements are indeed also present for the 4*d* elements, as for example, the rather drastic change of screening for the elements beyond the noble metals. However, this change of screening is not immediately obvious from Fig. 6 because of the differences in the free-atom configuration in Pd, Ag, and Cd. It is only when we consider the ΔE_c^{II} and ΔE_c^{I} shifts that this feature becomes clearly displayed. This comparison is postponed to the summary section. Indeed, due to the zero-valent, monovalent, and divalent free-atom configurations for Pd, Ag, and Cd, respectively, their ΔE_c shift in Fig. 6 looks very much the same. *Relative to the free-atom configuration* the final-state screening is dominated by *s*-electron screening in Pd and Ag and *p*-electron screening in Cd. From this alone one would expect a larger ΔE_c shift for Pd and Ag than for Cd. However, for Ag (as previously for Cu) this difference in screening is outweighed by the initial state effect that the *d* electrons contribute to the bonding in Ag but not in Cd. In the case of Pd the *d* electrons are bonding both in the initial and the final state, but more effectively so in the initial state. This circumstance reduces the ΔE_c shift for Pd so that it becomes comparable to the shift for Ag. Finally, we would like to bring to the reader's attention the fact that Pd is unique among the transition-metal atoms in having a closed-shell free-atom configuration (d^{10}). Therefore, the core-electron spectrum should be particularly simple to analyze and interpret for this atom.

VI. 5*d* TRANSITION ELEMENTS

For the metallic elements of the sixth period there are experimental data available for Cs, Ba, Yb, Hg, Tl, Pb, and Bi.[62] However, for the 5*d* elements, Lu–Au, there is no experimental information for the free atoms. Nevertheless, it turns out that it is possible to calculate accurate atomic binding energies for the $4f_{7/2}$ level (from Yb to Hg). The details of these calculations are accounted for in the Appendix. Further, a rather appropriate value for the $5p_{3/2}$ atomic excitation in La can also be derived (see Appendix). Thus it is possible to obtain good quasiexperimental data[86] also for the 5*d* elements. In Fig. 7 we compare these shifts with

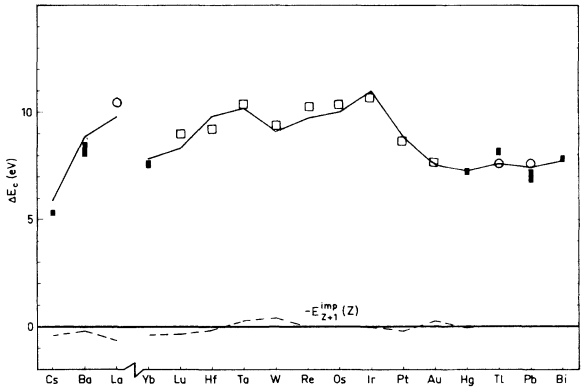

FIG. 7. The full line is the calculated core-level binding-energy shift, Eq. (7), for the metallic elements in the sixth period (excluding most of the lanthanides). The experimental and the two types of pseudoexperimental data have the same notation as in Figs. 3 and 6. The open circles refer to the $5p_{3/2}$ (La) and the $5d_{5/2}$ shifts (Tl, Pb); open squares refer to the $4f_{7/2}$ shifts. The dotted line is the impurity contribution to the shift.

those derived from Eq. (7), and, as for the other transition series, a good agreement is found. The general behavior of the level shift from Yb to Bi is most reminiscent of the ΔE_c shifts in the 3*d* and 4*d* series, which of course, is nothing but a confirmation of the chemical periodicity of the elements. The dip between Ir and Pt is due to the monovalent configuration, d^9s, in atomic Pt. It should be mentioned that the first ionization potential has not, as yet, been accurately determined for some of the 5*d* elements,[60] which adds some uncertainties to our calculated shifts.

In a previous work[76] the 4*f* electron excitation energies for the lanthanide metals were treated in very much the same manner as the $E_{c,F}^{M}$ energies in the present work. Thereby a very good agreement with experiment was obtained. In the present work we have shown that the binding energy of the 4*f* level can be understood also for the 5*d* metals (Yb–Hg) as well as for Tl, Pb, and Bi. Thus the 4*f* excitation energy can be quite accurately accounted for in a sequence of 26 metals.

In Fig. 7 we have for Tl included both an experimental (based on the 4*f* levels) and a pseudoexperimental point (based on the $5d_{5/2}$ level). Since the $E_{Z+1}^{imp}(Z)$ term is quite small in this region of the sixth period, we expect the calculated ΔE_c shifts to be particularly accurate for these elements. Tl, for instance, forms almost an ideal solid solution with Pb (the $Z+1$ element). One would, therefore, expect the experimental point for Tl to be very close to our ΔE_c curve. The estimated errors in the solid-phase core-level binding energies cannot alone explain the dis-

crepancy seen in Fig. 7. The calculated ΔE_c value is, furthermore, supported by the pseudo-experimental point which was based on the $5d_{5/2}$ level. The results, therefore, indicate that the Tl $4f$ excitation series limits determined in Ref. 26 might be somewhat too high. Also for Pb we have in Fig. 7 added a pseudoexperimental point based on the calculated atomic $5d_{5/2}$ binding energy in Table VIII[69(b)] and the experimental solid-phase binding energy from Ref. 88. As for Tl, a good agreement with the calculated ΔE_c shift (7.44 eV) is obtained for the $5d$ level. However, combining the atomic $4f_{5/2,7/2}$ binding energies from Ref. 28 (148.5 and 143.6 eV) with the solid-phase values from Ref. 88 [141.69(10) and 136.85(10) eV], a shift of only 6.8 eV is obtained (corresponding to the lower part of the dark bar in Fig. 7). Thus the experimental atomic binding energies[28] seem, in this case, to be somewhat low. Further, a direct inspection of the experimental shifts for Hg–Bi in Fig. 7 (the dark bars) shows that there is a rather large irregular variation. This is, however, physically somewhat unreasonable, indicating some slight inconsistencies in the experimental data (see Appendix for a further discussion on these matters).

The difference in screening (Fig. 7) between Ba and Yb as well as between La and Lu, can be understood from the lanthanide contraction. The insufficient $4f$ electron screening of the increased nuclear charge in Lu as compared to La causes a contraction of the valence orbitals. In a relative sense, however, the $6s$ orbital contracts more than the $5d$ orbitals, thereby increasing the $6s$ electrons' screening of the $5d$ orbitals, while the $5d$ electron screening of the $6s$ orbital decreases. Indeed, the "d-ionization" energy corresponding to the reaction $ds^2 \rightarrow (s^2)^{+1}$ is 6.49 eV for La and reduced to 5.43 eV for Lu (Ref. 59). Thus the d electrons are somewhat less bound for the heavier lanthanides than for earlier elements, which explains the decrease in the ΔE_c shift through the lanthanide series.

VII. $4f$ AND $5f$ TRANSITION METALS

The electrons in the open $4f$ shell of the lanthanides retain their atomic properties in the metallic phase and give rise to localized magnetic moments.[90,91] From this point of view the $4f$ electrons can be treated on the same footing as the other core electrons. This core-electron property of the $4f$ shell was the basic assumption in a recent treatment of the $4f$ excitation energies in the rare-earth metals.[76] The obtained agreement with experiments strongly supports this localized picture of the $4f$ levels. As far as the other core levels are concerned, we will for simplicity here, limit ourselves to those inner shells which are spatially more confined than the $4f$ orbitals. Further, we will also neglect the multiplet splitting between the two open shells, namely, the core-ionized c shell and the f^n configuration.[92] For very deep core levels these multiplet splittings will be rather small. In Fig. 8 we show the calculated binding-energy shifts ΔE_c for the $4f$ transition metals.[93] The most significant feature of this figure is the deviating behavior found in the metals Pr–Sm and Tb–Tm. The reason for this is the fact that for these elements the atomic configuration is of a divalent type,[59] $f^{n+1}s^2$, while the metallic state is trivalent,[91] $f^n(ds)^3$. Thus there takes place a considerable redistribution of the electronic structure when these atoms condense to the solid phase. Also, europium and ytterbium are divalent in the gas phase. However, these two elements remain divalent in their metallic phase, which explains their regular values of the ΔE_c shifts. The remaining lanthanides (La, Ce, Gd, and Lu) are trivalent both in the atomic and metallic phase, and therefore their ΔE_c shifts show normal behavior.

It has become a standard statement that the core electrons are more bound in the gas phase than they are in the metallic phase. The fundamental reason for this is the final state screening by the surrounding conduction electrons in the metal. Here we will investigate if this statement also holds true for the lanthanides. In order to do that we must, of course, use the *same* reference level for the binding energies involved. Therefore, we should use the δE_c shift defined in Eq. (3), which means that we have to account for the metal work function. The work function is

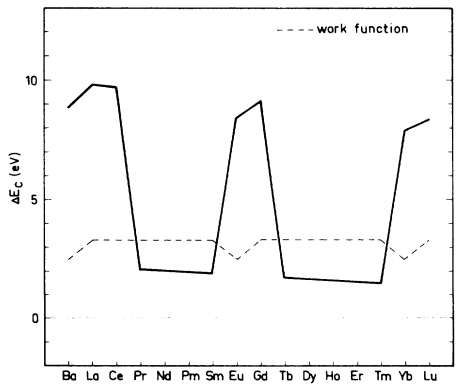

FIG. 8. Calculated binding-energy shifts ΔE_c for the lanthanide elements (Ba is also included). The core orbital c refers to a more localized orbital than the $4f$ orbitals. The work function is denoted by a dotted line and is discussed in the main text.

3.3 eV for lanthanum,[2] which should also be a rather appropriate value for the other trivalent lanthanides. This is shown as a dotted line in Fig. 8. For the divalent metals, Eu and Yb, we have used the work function[2] for Ba, 2.5 eV. From Fig. 8 it now becomes clear that for those lanthanides which change valence upon condensation, the δE_c values are *negative*. Thus we meet the rather remarkable situation in which the core electron is more bound in the metal phase than in the free atom. The reason for this is, of course, the fundamental difference in electronic structure between the atomic and the metallic phase for these elements.

In order to treat all the metallic elements in the Periodic Table we will here, for completeness, also include the actinide elements.[94] However, due to lack of experimental values of the cohesive energy for many of these elements[96] as well as lack of some crucial spectroscopic data,[97-100] the calculated shifts shown in Fig. 9 should be regarded as rather tentative. Further, we have also for simplicity only considered shells more localized than the $5f$ orbitals. For the heavier rare-earth-type actinides ($\geq$Am) we note a similar type of behavior as for the lanthanides, namely, a pronounced dip for Am, Bk, and Cf. These elements are divalent as atoms but trivalent in the metallic phase.[91,101-103] For the actinide elements beyond Cf the ΔE_c shifts behave in a regular manner, since there is no valence change upon the condensation to the metallic phase.[104] For the earlier actinides the situation is much more complex. Here, it is likely that a deep core hole will be predominantly screened by $5f$ electrons. Some most interesting screening situations can be envisaged for some of these elements, but since there are no atomic-core-level binding energies available for the moment, we feel that a further elaboration on this might become somewhat too academic. We only comment on that the irregularities of the ΔE_c shifts for the earlier actinides originate mainly from the large differences between the electronic structure of the atoms and the metals.

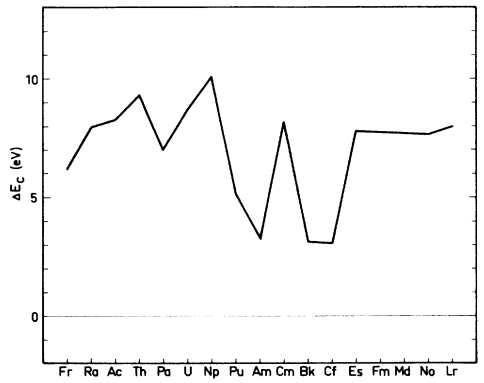

FIG. 9. Calculated binding-energy shifts ΔE_c for the actinide elements (also included are Fr and Ra).

VIII. $5f$ OCCUPATION IN URANIUM METAL

The electronic structure of the lighter actinide metals has been a problem under long-standing debate and controversy. Only recently has it become rather commonly accepted that the $5f$ level is occupied in uranium and that the $5f$ electrons have itinerant (band) properties.[107-109] The previous picture was that uranium is a hexavalent metal of type $(6d7s)^6$ with no occupation of the (assumed) localized $5f$ level.[110,111] Thus uranium was considered to be the actinide analog to molybdenum and tungsten in the $4d$ and $5d$ series, respectively. This conclusion was drawn mainly from the metallic radius and the chemical properties of uranium. However, there are many other properties of metallic uranium which indicate that its electronic structure cannot be that simple.[112] We are not going to discuss this question in detail here, but will just investigate which of these pictures the measured core-level binding energies favor.

In the course of the present investigation we were led to consider the metallic binding energy of a particular core level c as a function of the atomic number. Not unexpectedly, a quite regular behavior could thereby easily be distinguished. This holds in particular, for the outermost p level of the core and in Fig. 10 we have plotted the $2p_{3/2}$, $3p_{3/2}$, $4p_{3/2}$, and $5p_{3/2}$ metallic binding energies for the earlier elements in the third–sixth period, respectively.[113] From this figure, the mentioned regularity is evident, as well as a relatively smooth lowering of the p-level binding energy with increasing period.

If we consider the $5p_{3/2}$ level for Cs, Ba, and La, we note that the regular pattern seen in the other periods is broken when we arrive at the lanthanide elements. Thus, although the Z number has increased by 14 when proceeding from La to Lu, the $5p_{3/2}$ binding energy has increased by only 10 eV. This is, of course, due to the filling of the $4f$ level. Since the $4f$ orbital is spatially much more localized than the $5p$ orbital, the $4f$ shell electrons screen very effectively the increased nuclear charge, which would otherwise strongly attract the $5p$ electrons. However, this screening is not quite perfect, which is evident from the fact that the $5p_{3/2}$ level is more bound in Lu than in La.

With this introduction we are now prepared to consider the case of uranium. Let us now assume that the uranium metal is of $(sd)^6$ type like Mo

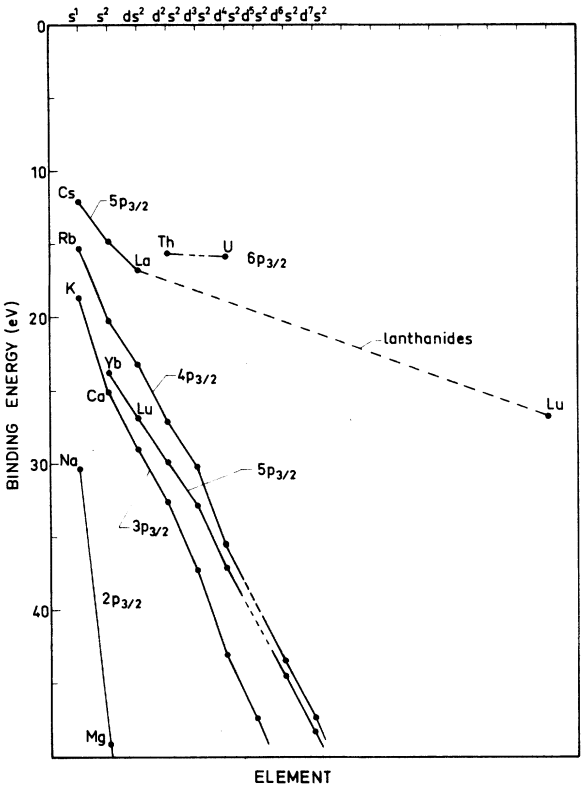

FIG. 10. Experimental binding energies, $E^{M}_{c,F}$, of the $2p_{3/2}$–$6p_{3/2}$ core levels for elements in the left part of the Periodic Table. The labeling of the horizontal axis by s and $d^n s^2$ ($n = 0, 1, \ldots$) just represents the columns (1A, 2A, 3A, ...) of the Periodic Table.

and W. Even so, it might be that the screening of a core hole in uranium is different from what it is in Mo and W, namely, that the main screening charge is of $5f$ type. However, for the $6p_{3/2}$ core hole this could not be the case since this core hole is situated *outside* the $5f$ orbital. Thus for a $6p_{3/2}$ core hole in (hypothetical) $(sd)^6$ uranium, the screening property should closely correspond to that in Mo and W. The thorium metal is of normal tetravalent $(sd)^4$ type and the screening of a $6p_{3/2}$ hole should, therefore, be comparable to that in Zr and Hf. Thus, with the assumption of an $(sd)^6$ uranium metal, we expect the same pattern of the $6p_{3/2}$ binding energy in the beginning of the actinide series as for the outermost p levels in the $3d$–$5d$ metals. However, as is clear from Fig. 10, this is far from being the case. Instead, the $6p_{3/2}$ electrons in uranium are much less bound than expected for an $(sd)^6$ transition metal. In view of the behavior of the lanthanides, the reason for this is clear. Uranium metal has to have an appreciable occupation of the $5f$ level (about two electrons). These electrons screen the nuclear charge seen by the $6p$ electrons, thereby causing a substantial reduction of the $6p_{3/2}$ binding energy.

In order to quantify the discussion above, we have calculated the $6p_{3/2}$ ionization energy for atomic thorium ($6d^2 7s^2$ configuration) and atomic uranium (hypothetical $6d^4 7s^2$ configuration), thereby obtaining the values 25.8 and 31.3 eV, respectively (see Appendix). For thorium we have estimated the $I^{Z+1}_{(Z)}$ term to be 7.4 eV. From a comparison with zirconium and hafnium, the cohesive energy terms in Fig. 1 are found to give an extra contribution to the level shift of about 1.5 eV. Thus we calculate the $6p_{3/2}$ binding energy in metallic thorium to be $25.8 - 7.4 - 1.5 = 16.9$ eV. This value is in satisfactory agreement with the experimental value[114] of 16.6(3) eV. In the case of uranium an appropriate value for the hexavalent metallic shift should be about 9–10 eV. Thus hexavalent metallic uranium should have a $6p_{3/2}$ binding energy higher than 21 eV. However, the experimental value[114] is 16.8(5) eV. This clearly shows the inadequacy of the hexavalent picture for uranium.

Thus, in conclusion, the measured value of the $6p_{3/2}$ binding energy in metallic uranium definitely supports the view that there is a substantial occupation of the $5f$ level. Then, in order to understand for example, the small metallic radius of uranium, these f electrons must be considered as actively taking part in the bonding of the metal.[115-120] This is indeed the case for the itinerant picture of the $5f$ electrons.[121,122]

IX. SURFACE CORE-LEVEL SHIFTS

Surface atoms experience a potential different from the bulk due to the lower coordination number. From this it is clear that one should expect a somewhat different core-level binding energy for the surface atoms as compared to the bulk atoms. Experimentally, however, the situation has been rather controversial, and it is only very recently that unambiguous surface core-level shifts have been observed.[123-125] A theoretical account for some of these shifts has already been given in Ref. 106.

The present formulation of the core-level binding energies can rather easily be generalized to the surface situation. For a surface atom all the arguments leading to Eq. (4) [and its approximate form Eq. (6)] can be repeated, but the bulk cohesive energies should be replaced by surface cohesive energies[126] and the impurity term should refer to a situation with a surface impurity.[127] Thus we obtain the core-level binding energy for a surface atom, $E^{M\,\mathrm{surf}}_{c,F}$, as [within the $(Z+1)$ approximation]

$$E_{c,F}^{M\,\mathrm{surf}} = E_{\mathrm{coh,surf}}^{Z} + E_{c}^{A} - I_{(Z)}^{Z+1} - E_{\mathrm{coh,surf}}^{Z+1} + E_{Z+1}^{\mathrm{imp,surf}}\ (Z), \tag{9}$$

where $E_{\mathrm{coh,surf}}^{Z}$ is the surface cohesive energy of the Z metal and $E_{Z+1}^{\mathrm{imp,surf}}\ (Z)$ is the solution energy of the $(Z+1)$ impurity at the surface of the Z metal.[127] From experimental surface tension measurements it has been found that *empirically* the surface cohesive energy is related to the bulk cohesive energy as[128,129]

$$E_{\mathrm{coh,surf}} = 0.8 E_{\mathrm{coh}}. \tag{10}$$

Skapski[130,131] has theoretically derived a similar relation from considerations of the number of broken bonds for a surface atom as compared to a bulk atom. This picture of broken bonds for the surface energy has been severely questioned by Evans.[132] Here, however, we will only use Eq. (10) as an empirical relation. Furthermore, it seems most plausible that the impurity term should also obey a similar (empirical) relation, namely,

$$E_{Z+1}^{\mathrm{imp,surf}}\ (Z) = 0.8 E_{Z+1}^{\mathrm{imp}}(Z). \tag{11}$$

It should be emphasized that the relation (10) is derived from surface tension data for the metallic liquid phase, *extrapolated* to low temperature (and crystalline structure). However, the coordination number for an atom at the surface of the liquid might be quite different than for the crystalline phase. At best, the liquid surface coordination number may correspond to the average of the different types of surfaces possible for the crystalline phase. This "average property" has to be borne in mind when the simple relations in Eqs. (10) and (11) are applied to specific cases.

Equations (6) and (9)–(11) can easily be combined so that we obtain a simple expression for the core-level binding-energy shift between the surface and the bulk, $DE_{c}^{S,B}$ (B = bulk, S = surface). This reads

$$DE_{c}^{S,B} = E_{c}^{\mathrm{surf}} - E_{c}^{\mathrm{bulk}} = 0.2[E_{\mathrm{coh}}^{Z+1} - E_{\mathrm{coh}}^{Z} - E_{Z+1}^{\mathrm{imp}}(Z)]. \tag{12}$$

Thus the core-level surface shift is approximately 20% of the absorption shift Δ_a in Eq. (8). Note that the above treatment gives a direct relation between the surface chemical shift and the heat of surface segregation of a $(Z+1)$ substitutional impurity in the Z metal.

In Fig. 11 we plot the calculated surface atom core-level shifts for the 5*d* elements. The most salient feature is the change of sign of the surface shift near the middle of the series. Thus, for the earlier transition elements the core level is more bound at the surface than in the bulk, while in the latter part of the series the reverse situation is met with. This can be understood as follows: The final-state valence-charge distribution around the core hole is essentially that of the $(Z+1)$ element. For elements in the beginning of the transition series this means that the binding due to the conduction electrons is stronger in the final state than in the initial state. This is so, since, for these earlier *d* elements the $(Z+1)$ screening takes place in the bonding part of the *d* band. For the heavier elements with a half-filled or more than half-filled *d* band the situation is the opposite. [Here the $(Z+1)$ screening utilizes the antibonding part of the *d* band.] Therefore, for the earlier *d* metals, the gain in bonding in the final state is larger for a bulk atom than for a surface atom, due to the larger coordination number in the bulk. This immediately explains the increased core-level binding energy for the surface atoms for these metals. For the heavier *d* metals the situation is reversed.

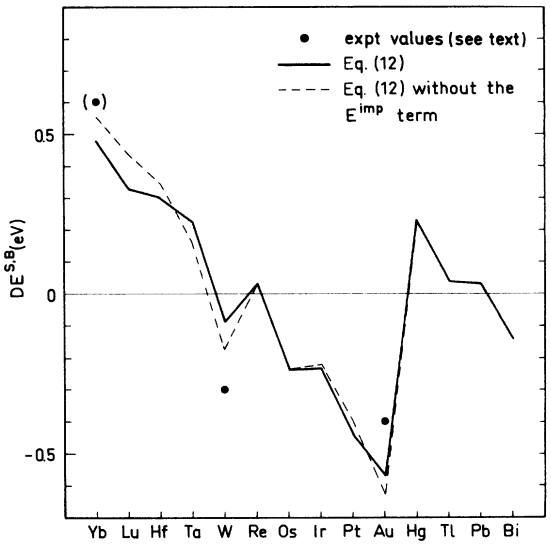

FIG. 11. Calculated surface atom core-level shifts relative to the bulk for the elements Yb–Bi in the sixth period. The experimental data are from Refs. 123, 125, and 133. The parentheses for Yb is used to indicate the somewhat uncertain origin of this value (see text and discussion in Ref. 134).

From Fig. 11 it is rather interesting to note that a similar change in the sign of the surface atom core-level shift also takes place in the middle of the 6*p* series (Hg–Rn). The same arguments as given above for the 5*d* elements can be applied here, and therefore, the change of sign of the surface shift just reflects the bonding-antibonding division of the *p* band. In Fig. 11 we have included two experimentally determined surface atom core-level shifts. This is for the (110) surface of W (Ref. 125) and for

the surface of evaporated Au films > 1000 Å thick.[123] In the case of Yb an increased surface core-level binding energy of 0.6 eV has been reported,[133] but the authors of Ref. 133 believe this to be due to surface contamination of oxygen. Here we conjecture that this observed shift could originate equally well from the surface effect[134] and we have included this value into Fig. 11. (In view of the uncertainty of its origin we have put this value within parentheses, however.) Since the relation for the surface cohesive energy in Eq. (10) probably only expresses a rather crude (and an averaged) estimate, one might consider the agreement between our calculated surface core-level shifts and the experiments, to be quite reasonable. (See also notes added in proof.)

From the given description it follows that for an individual element one would expect the largest surface atom core-level shift for that surface plane which has the lowest coordination number. From the simple bond-breaking picture one would also expect a linear relation between the surface coordination number and the surface level shift. However, this linear effect should be partly compensated by the tendency of the individual bonds to strengthen somewhat when the coordination number is lowered. For a metal like plutonium, whose properties already in the bulk are most sensitive to the coordination number, one might expect a quite pronounced dependence of the surface atom core-level binding energy on the surface plane direction. Another most interesting case is samarium, which is a trivalent metal in the bulk, but appears to be divalent at the surface.[135-137] From Fig. 8 we note that for a surface samarium atom this will have a dramatic effect on the binding energies of the deep-core electrons and a decrease of nearly 7 eV as compared with the bulk should be expected. For the $3d$ core electron spectra, whose spin-orbit components are multiplet splitted over a range of about 3–4 eV, Wertheim and Crecelius[135] observe a surface shift of 7.6 eV.

When comparing the surface core-level shift between different metals, one would expect the largest shift for those metals whose properties are most different from that of its next following element in the Periodic Table. From this point of view the observed large surface core-level shift in gold seems quite fitting, since the element after gold, mercury, indeed has properties quite distinguished from those of gold.

X. RARE-GAS ATOMS IMPLANTED IN NOBLE METALS

Accurate experimental core-level binding energies are available for the free rare-gas atoms.[138] Previously, Citrin and Hamann[18] as well as Watson, Herbst, and Wilkins[144] have considered the physical situation of having rare-gas atoms implanted in noble metals. Both these studies successfully reproduced the experimental trends of the implanted rare-gas atom core-level shifts, and the work by Watson *et al.* even gave a good numerical agreement. However, as stressed by Watson *et al.*, both their approach and that of Citrin and Hamann encompass rather drastic simplifying assumptions and neither can be unambiguously asserted to be unique. Here we address ourselves to the same problem, applying a simple generalization of the approach outlined in Sec. II. As will become evident below, the present method is unfortunately hampered by lack of certain crucial data. However, instead of trying to verify the applicability of the present approach, we will here assume that it contains all the essential contributions to the core-level shift, and from this, derive data which might otherwise be difficult to obtain.

In Fig. 12 we show the Born-Haber cycle which applies to the present case of implanted rare-gas atoms. The first step involves the energy required to implant a rare-gas atom into the metallic host of atomic number Y. This energy will be denoted by $E^{\text{implant}}(Y)$. In the next step we proceed from the free rare-gas atom to the core-ionized state, a process which defines the energy E_c^A. This core-ionized state is then replaced by an almost equivalent one, namely, the $(Z+1)$ alkali +1 ion. The remaining steps in the cycle are very similar to those in Fig. 1. The only difference is that in the last step a $(Z+1)$ metal site is dissolved into the Y metal. This gives the solution energy $E_{Z+1}^{\text{imp}}(Y)$. Thus we

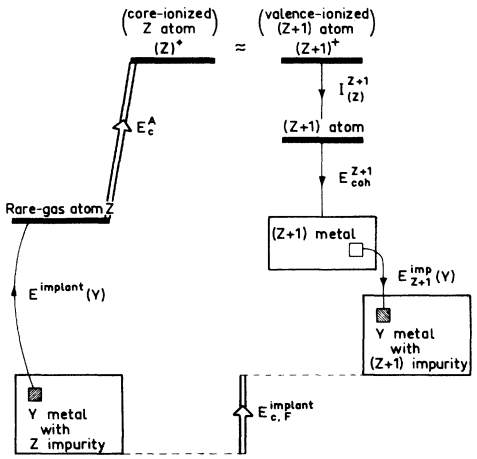

FIG. 12. Born-Haber cycle for the implanted rare-gas core-level binding energy $E_{c,F}^{\text{implant}}$ in a metal Y. Its construction is described in the text.

obtain the following binding energy of the core level labeled c for an implanted rare-gas atom:

$$E_{c,F}^{\text{implant}} = E^{\text{implant}}(Y) + E_c^A - I_{(Z)}^{Z+1} - E_{\text{coh}}^{Z+1} + E_{Z+1}^{\text{imp}}(Y). \tag{13}$$

The corresponding shift is then given by

$$\Delta E_c^{\text{implant}} = E_c^A - E_{c,F}^{\text{implant}}$$
$$= I_{(Z)}^{Z+1} + E_{\text{coh}}^{Z+1} - E^{\text{implant}}(Y) - E_{Z+1}^{\text{imp}}(Y). \tag{14}$$

For the impurity term, $E_{Z+1}^{\text{imp}}(Y)$, we apply the Miedema scheme. Thus, except for the implantation energy, all quantities on the right-hand side of Eq. (14) are known. These terms are listed in Table I together with the experimental $\Delta E_c^{\text{implant}}$ energies. By assuming the validity of Eq. (14) we may now *derive* values for the implantation energy, $E^{\text{implant}}(Y)$. The obtained values are also given in Table I. Since the size of the rare-gas atom is likely to be relatively independent of the host, this means that in a relative sense the rare-gas atom will introduce the largest disturbance in the metal having the highest number density (atoms/cm^3), i.e., in copper. This view is confirmed by the derived numbers. Similarly, for a given host metal the largest disturbance should be expected for the largest rare-gas atom. This expected trend is also exhibited by the derived values of E^{implant}. The only deviation is observed for Ar implanted in Ag and Au. However, these binding energies have been measured by another group,[146] and they obtained 241.9 eV for Ar in Ag, and 240.5 eV for Ar in Au. With these binding energies we get 1.8 eV for the implantation energy of Ar in Ag, and 2.4 eV for Ar in Au. If we use these values in Table I the implantation energy does increase in all cases with increasing size of the rare-gas atom. These differences, however, also show that the errors in the observed binding energies might be quite large (several tenths of an eV). As regards the appropriateness of the magnitude of the obtained implantation energies, it is more difficult to make an assessment. The only comparable case we are aware about is a theoretical study of the implantation energy of a helium atom in silver.[147] For this case the calculated implantation energy was found to be 1.5 eV. In comparison with the currently derived rare-gas implantation energies in Ag, this value seems rather fitting, especially so since helium is the smallest rare-gas atom. Besides possible experimental difficulties, the main uncertainty in the present approach is probably due to the impurity term, $E_{Z+1}^{\text{imp}}(Y)$. From Table I we note that the Miedema solution energies for alkali impurities in noble metals can attain rather large values, and therefore the relative error might be quite large.

XI. DISCUSSION AND SUMMARY

In Secs. I–X we have compared the calculated core-level shifts with experimental as well as pseudoexperimental values. In Fig. 13 we summarize this comparison in an extension of Fig. 2.

TABLE I. Summary of quantities used in the Born-Haber cycle [(Eq. (14)] for implanted rare-gas atoms in Cu, Ag, and Au. $E_{c,F}^{\text{implant}}$ is the binding energy for the implanted atom relative to the Fermi level, E_c^A is the corresponding binding energy for the free rare-gas atom relative to the vacuum level, $\Delta E_c^{\text{implant}}$ is the difference between these two binding energies, $I_{(Z)}^{Z+1}$ is the neutralization energy within the $Z+1$ approximation, E_{coh}^{Z+1} is the cohesive energy for the $Z+1$ alkali metal, $E_{Z+1}^{\text{imp}}(Y)$ is the solution energy (within Miedema's semiempirical scheme) of the $Z+1$ alkali metal impurity in the host metal (Cu, Ag, or Au), and finally $E^{\text{implant}}(Y)$ is the calculated energy [(Eq. (14)] associated with the implantation of a rare-gas atom in the host metal.

Host metal	Implanted atom	$E_{c,F}^{\text{implant}}$ a	E_c^A b	$\Delta E_c^{\text{implant}}$	$I_{(Z)}^{Z+1}$	E_{coh}^{Z+1}	$E_{Z+1}^{\text{imp}}(Y)$	$E^{\text{implant}}(Y)$
Cu	Ne	862.18	870.21	8.03	5.14	1.11	0.45	2.23
	Ar	241.09	248.63	7.54	4.34	0.93	1.03	3.30
	Kr	207.27	214.55	7.28	4.18	0.85	1.16	3.41
	Xe	669.58	676.70	7.12	3.89	0.80	1.31	3.74
Ag	Ne	862.38	870.21	7.83	5.14	1.11	−0.01	1.57
	Ar	241.19	248.63	7.44	4.34	0.93	0.31	2.48
	Kr	207.60	214.55	6.95	4.18	0.85	0.36	2.28
	Xe	669.62	676.70	7.08	3.89	0.80	0.42	2.81
Au	Ne	861.56	870.21	8.65	5.14	1.11	−0.54	1.86
	Ar	240.26	248.63	8.37	4.34	0.93	−0.41	2.69
	Kr		214.55		4.18	0.85	−0.43	
	Xe	668.89	676.70	7.81	3.89	0.80	−0.45	2.67

[a] From Ref. 18.

[b] See Ref. 145.

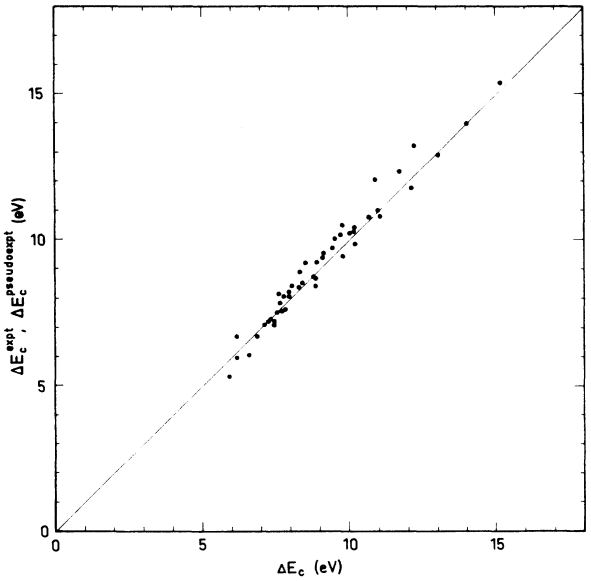

FIG. 13. Comparison between the experimental, ΔE_c^{expt}, as well as pseudoexperimental, $\Delta E_c^{\text{pseudoexpt}}$, and the theoretical, ΔE_c, core-level binding-energy shifts. For clarity the average position of the bars in Fig. 2 has been used.

The overall good agreement shows that the given description of a core ionization in a metal contains the essential contributions. In particular, this must mean that the complete screening picture of the core hole is indeed appropriate for metals. The question then arises as to what extent a similar picture is applicable to semiconductors and insulators. For semimetals and small-band-gap semiconductors it seems resonable to expect that a core hole here should also become totally screened.[148] For insulators, however, the situation should be different. Here the surrounding medium will give rise to a polarization field around the core hole, but there are no carriers available to locally screen the ionized site. Thus, for semiconductors, there might be a critical value of the energy gap, above which free-carrier screening is no longer possible.

Not unexpectedly, a regularity was found in the core-level shifts, which directly reflects the chemical periodicity of the elements. However, this might be somewhat obscured by "accidental" differences in the atomic ground-state configurations. This is especially the case for the $4d$ elements. Therefore, we give in Fig. 14 the calculated level shifts for the divalent and monovalent configurations of the d-transition-series elements as discussed in connection with Fig. 4 in Sec. IV. In Fig. 15 we make a direct comparison between the divalent and monovalent shifts, ΔE_c^{II} and ΔE_c^{I}, for the different periods and we

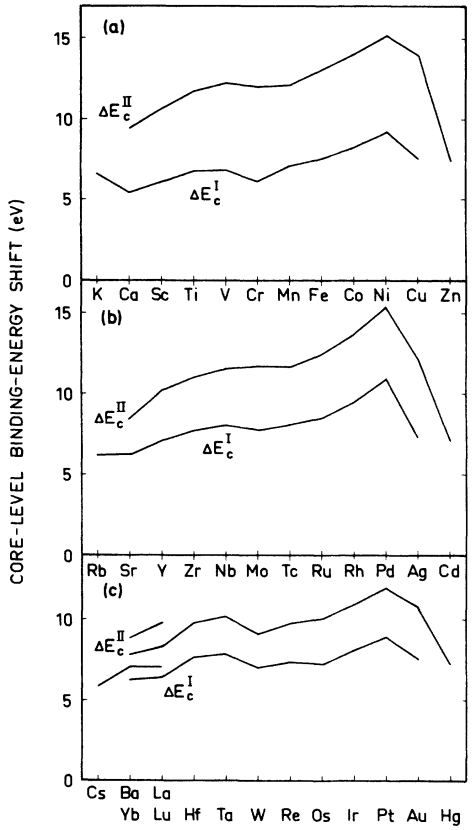

FIG. 14. Calculated monovalent (ΔE_c^{I}) and divalent (ΔE_c^{II}) shifts for the $3d$–$5d$ elements.

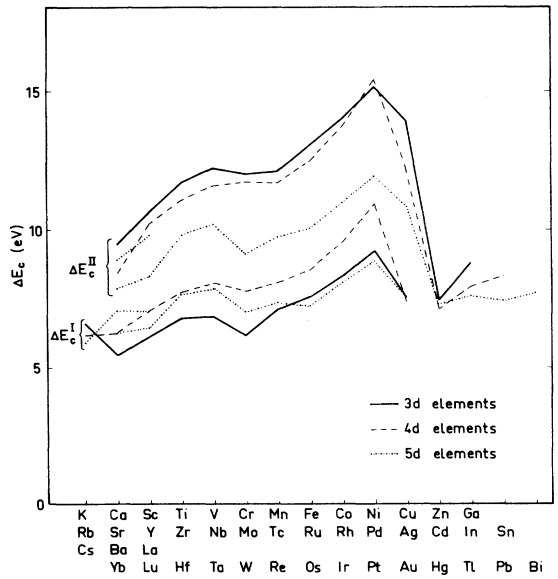

FIG. 15. Comparison between the monovalent and divalent shifts for the $3d$–$5d$ elements. Also the shifts for the other metallic elements in the fourth–sixth period are included.

also include the "p transition" metals. From this figure the periodic variation of the level shifts can easily be identified.

The present approach was made possible thanks to the Born-Haber cycle shown in Fig. 1. However, it is only after the introduction of the $(Z+1)$ approximation that the scheme becomes practically useful. The $(Z+1)$ approximation for the ionization energy, I^{Z*}, might in some cases introduce a significant error. This point will be investigated in a future communication, where we will study to what extent the $(Z+1)$ approximation depends on the particular core level c accommodating the hole.[54] Still, we feel that occasionally the largest error might be due to the impurity term, $E_{Z*}^{\mathrm{imp}}(Z)$. For this quantity it seems, however, unlikely that the $(Z+1)$ approximation, $E_{Z+1}^{\mathrm{imp}}(Z)$, should cause any significant error. Instead it is the Miedema semiempirical scheme for the $(Z+1)$ impurity problem itself, which in certain cases might very well be erroneous. However, the solution energy, $E_{Z+1}^{\mathrm{imp}}(Z)$, can in principle be obtained from experiment, and one might hope that in the future, experimental values will become more frequently available than at present. On the other hand, it is only quite recently that the Miedema scheme has become widely recognized, and, as more and more experience is gained from its application to various physical and chemical situations, its eventual limitations for specific cases will become mapped out.

As regards the experimental metallic core-level binding energies, one often finds unreasonably large deviations between different investigators. The main reason for this seems to be that insufficient attention has been paid to the calibration problem. This is explained by the fact that, often, the absolute value of the binding energy has not been the primary interest of the experiment, but rather some special feature of the spectrum for which a careful calibration certainly is not necessary. Thus the scatter of the experimental values is not usually due to limitations of the experimental technique. Therefore, increased attention to the calibration problem could, in most cases, easily improve on this currently somewhat unsatisfying situation.

Naturally, it is experimentally much easier to determine core-level binding energies for the metallic state than it is for the free atom. Most certainly, it will take a long time before core-level binding-energy data for the free atoms will become available to the same extent as they are today for the metallic phase. In this situation it seems most valuable if relatively accurate data for the free atoms could be provided by some indirect means. Having demonstrated the reliability of the present method for the core-level shifts, it thus becomes possible to derive atomic binding energies from the experimental data of the corresponding metal. This will be done in a forthcoming article.[54]

The insight gained into the origins of the core-level shifts permits a confident study of the regularity of the metallic binding energy of the outermost p core shell. In particular, this means that if the earlier actinides were of normal d-transition metal character, the core-hole screening should be very similar to the one in the $3d$, $4d$, or $5d$ series. From this we could show that the experimental binding energy of the $6p_{3/2}$ level in uranium metal definitely indicates that there must be an appreciable occupation of the $5f$ state. Thus uranium is not a simple d-transition metal but has a more complicated electronic structure.

The present approach easily lends itself to generalizations so that systems other than the pure metals can be considered. In this paper we chose the case of implanted rare-gas atoms in noble metals to give an illustration of how this can be done. In this particular case we used the experimentally determined core-level shifts to indirectly derive thermodynamic data, which otherwise might be quite difficult to obtain. At this stage it is, however, somewhat difficult to assess the accuracy of the obtained results. The main reason for this is the uncertainties which might be impaired to the Miedema values for the impurity term. As more experience will be gained, however, it seems possible that measured core-level shifts can become a useful means to obtain thermochemical information. A generalization to dilute alloys and more complicated systems will be presented in a future publication.[149]

There is one further comment which might be worth making in connection with the core-level shifts for implanted rare-gas atoms. It has been argued (e.g., in Ref. 146) that these shifts can be used to probe the capability of the host metal to shield a core hole in the metal. One thus regards the "extra-atomic relaxation" mainly as a property of the surrounding metal. The obtained shifts are then used to separate initial- and final-state effects in the chemical shifts of alloys. As can be seen from Table I this assumption is clearly erroneous. The shift is mainly a property of the implanted atom itself (provided there is a metallic environment which can supply the screening electron to the final state). The influence of the particular metal on this shift is only included through the terms $E_{Z+1}^{\mathrm{imp}}(Y)$ and $E^{\mathrm{implant}}(Y)$. The latter term which in general seems to be the dominating one, is furthermore

a property of the initial state. The relatively constant value of the shift for a particular metal host (irrespective of the implanted rare-gas atom), which was the basis for the arguments in Ref. 146, is, therefore, mostly a consequence of the chemical similarity of the rare-gas atoms and thus an extension of the periodicity of the ΔE_c values which was demonstrated in Fig. 15.

At least in principle, one of the simplest chemical shifts is the core-level shift between a bulk and a surface metal atom. However, it is only very recently that such a shift has been observed experimentally. Relying on an empirical relation for the surface energy, we could derive a very simple expression for the surface shift. As a result, we found that, depending on the metal, the shift could be either towards higher or lower binding energies. Further, it seems most likely that the shift should be largest for the surface plane having the lowest coordination number.

Some time ago, a Born-Haber cycle similar to the one used in the present paper had been applied to describe the $4f$ excitation energies in the lanthanide metals.[150] A more refined treatment of these systems has now been given in Ref. 76. Also, Broughton and Perry[16] have recently treated core-level shifts by a method closely related to ours. However, they do not consider the cohesive energy terms in Fig. 1. Within a given period of elements (fourth, fifth or sixth) this means that their derived shifts will differ from ours by a total span of about 5–6 eV. A related treatment of core-level shifts for some molecules has been given by Jolly.[151] It is also well known that the Auger electron energies show a large shift between the free atom and the metal. For those Auger processes which end up in two holes in the core, an appropriately modified Born-Haber cycle can again be applied. A detailed account of this will be given in another publication.[152] Here we just mention that the agreement between experiment and theory is of the same quality as for the single core-holes in the present work.

To summarize, in this paper we have demonstrated that core-electron excitations in metals can be accurately described by a Born-Haber cycle. This confirms the complete screening picture of the core hole in the final state.

Notes added in proof. After completion of this work we became aware of the work by J. Reader, Phys. Rev. A 13, 507 (1976) who has studied the energy levels of Cs II. He found an ionization energy of 23.14 ± 0.02 eV in good agreement with our estimated value of 23.15(10) eV (Table V). Further, P. Mitchell [J. Phys. B 12, 1653 (1979)] has from Hartree-Fock calculations concluded that the $^2P_{1/2}$ level of the $5p^5 6s^2$ configuration should be revised. His new assignment gives a spin-orbit splitting of 12 240 cm^{-1} for this configuration. Thereby the mentioned anomaly in Ref. 162 is no longer apparent. From these two recent papers one derives a decoupled p-ionization energy of 17.42 eV, which is in good agreement with our calculated value of 17.44(2) eV. The Cs I spectrum has also been reinvestigated by J. P. Connerade, M. W. D. Mansfield, G. H. Newsom, D. H. Tracy, M. A. Baig, and K. Thimm, Philos. Trans. R. Soc. Lond. Ser. A, 290, 327 (1979).

Recently a positive surface chemical shift has been established for Ta [J. F. van der Veen, F. J. Himpsel, and D. E. Eastman, Phys. Rev. Lett. 44, 553 (1980)], thus verifying the predicted change in sign between Ta and W (see Fig. 11). Furthermore, for Ir the shift is found to depend on the surface atom coordination number in accordance with the suggestions in Sec. IX.

A recent reinvestigation of the Yb surface indicates that the observed shift (see Ref. 134) is indeed a true surface effect (L. Johansson, private communication).

ACKNOWLEDGMENTS

The authors are indebted to Dr. S.-E. Johansson for helpful comments on some optical atomic spectra. Also the private communications with Professor J. P. Connerade, Professor W. R. S. Garton, Professor W. Mehlhorn, Professor B. Sonntag, Professor N. P. C. Westwood, and Dr. L. Johansson are gratefully acknowledged. We would also like to thank Professor S. Aksela for communicating his results for silver prior to publication, and Professor M. Campagna for permitting us to quote the surface experiments for ytterbium prior to publication.

APPENDIX

As stressed several times in this paper, there is a substantial lack of experimental core-level binding-energy data for the free atoms. Further, for those cases where such data exist, it is usually only one or a few of the inner shell ionizations that has been measured. In such a situation it might seem quite reasonable to use calculated ionization energies instead. However, it is known that, for the moment, even the most extensive calculations give reliable results only for the very lightest elements. For the other elements, rather large discrepancies between theory and experiment are often found. Since in our present investigation an error larger than 0.5 eV is highly undesirable, we have to turn to other

methods. Below, we will introduce two different procedures which can be used for this purpose. In the first one, this is made possible by a combination of atomic calculations and experimental atomic spectroscopic data. In the second one, a kind of an interpolation is made between experimentally known ionization energies. For the atomic calculations we have employed the relativistic Hartree-Fock-Slater scheme, where we use the exchange parameter α as a free parameter. When we will refer to a calculated excitation energy later, note that this has always been obtained from a calculated total energy difference where the same α has been used for both the initial and the final state. It should be emphasized that we have been exclusively interested in finding a *practical* means for obtaining accurate core-ionization energies, and that we nowhere imply that the calculated atomic wave functions as such will faithfully represent the true wave functions.

A further complication arises for core ionizations in open shell atoms, namely, the multiplet splitting of the configuration made up by the core hole and the valence electrons. In view of the different spatial distributions of the core hole and the valence electrons, it seems appropriate to treat the core hole and the valence electrons as two separate systems whose total angular momenta, j_c and J_v, are coupled to form the total angular momentum J_T. This coupling is sometimes referred to as Jj coupling.[153] We illustrate this by considering the $2p$ core ionization in sodium. This leads to the following final-state possibilities[58]:

$$\mathrm{Na\,I} \rightarrow \mathrm{Na\,II} \begin{cases} 2p^5(j_c=\tfrac{1}{2})3s(J_T=0) & 38.462\ \mathrm{eV} \\ 2p^5(j_c=\tfrac{1}{2})3s(J_T=1) & 38.156\ \mathrm{eV} \\ 2p^5(j_c=\tfrac{3}{2})3s(J_T=1) & 38.081\ \mathrm{eV} \\ 2p^5(j_c=\tfrac{3}{2})3s(J_T=2) & 37.986\ \mathrm{eV}. \end{cases} \tag{A1}$$

In sodium metal this coupling is absent and only the spin-orbit splitting of the p level is observed. The way we calculate the excitation energy in the metal [the Born-Haber cycle in Fig. 1 combined with the $(Z+1)$ approximation] presupposes that the atomic ionization energy corresponds to the *decoupled* situation. In the case of sodium this means that a weighted averaging of the levels in Eq. (A1) has to be made before we arrive at the appropriate $E^A_{2p_{3/2}}$ to be used in our formula for the level shift, Eq. (7). As will become evident, the methods we are going to apply below are such that the derived values will directly correspond to the decoupled ionization energy.

In the following we will make an extensive use of data obtained from Ref. 60. Also Moore's Tables[58] and the recent compilation in Ref. 59 have been consulted. In addition to this, Refs. 154–160 and 61 have been utilized.

1. Method based on ionization potentials

This method utilizes the fact that for many elements quite a large number of ionization potentials are very accurately known.[60] This fortunate situation is particularly true for the lighter elements. However, for the heavier elements, the data are much less complete and for our present purpose only a few elements can be treated. The method itself is probably best described by an illustrating example. Let us consider magnesium and the $2p_{3/2}$ core ionization of this atom. Atomic magnesium has the ground-state configuration $(1s^2 2s^2 2p^6 3s^2)$, where the two electrons in the $3s$ orbital are the valence electrons. By ionizing magnesium to the ground state of the +3 ion, we arrive at the $(1s^2 2s^2 2p^2_{1/2} 2p^3_{3/2})$ configuration. This ion is then dressed by two electrons in its $3s$ orbital. Thus we end up with a +1 ion, $(1s^2 2s^2 2p^2_{1/2} p^3_{3/2} 3s^2)$, which is the desired $p_{3/2}$ core-ionized state. The discussion can be somewhat simplified if we consider the following two reactions which both lead to the same final state;

$$\mathrm{Mg}(s^2) \rightarrow \mathrm{Mg}^+ \rightarrow \mathrm{Mg}^{2+} \rightarrow \mathrm{Mg}^{3+}(p^3_{3/2}), \tag{A2a}$$

$$\mathrm{Mg}^+(p^3_{3/2}s^2) \rightarrow \mathrm{Mg}^{2+}(p^3_{3/2}s) \rightarrow \mathrm{Mg}^{3+}(p^3_{3/2}). \tag{A2b}$$

If the energies of these two reactions are known, we can directly obtain the $2p_{3/2}$ core-ionization energy. The energy in Eq. (A2a) is, of course, nothing but the sum of the first three ionization potentials for magnesium. The remaining problem is thus to find the energy of the reaction in Eq. (A2b). The two ionization steps from $\mathrm{Mg}^+(p^3_{3/2}s^2)$ to $\mathrm{Mg}^{3+}(p^3_{3/2})$ only involves the $3s$ valence electrons. This process is therefore, likely to be well described by its $(Z+1)$ substitution, namely, the double ionization of $\mathrm{Al}^+(s^2)$ to the Al^{3+} ion. However, since several ionization stages are involved, the relative error in this replacement can become rather substantial. To account for this, we start by calculating the energy for the $\mathrm{Al}^+(s^2) \rightarrow \mathrm{Al}^{3+}$ reaction and vary the value of the parameter α until the experimental value of 47.276 eV is obtained. This gives $\alpha = 0.8346$.

TABLE II. The $2p_{3/2}$ binding energies for the elements Na–Si, calculated with the method based on ionization potentials (method A). Columns 1–6 contain in the upper row the relevant ionization potentials for the Z atom and in the lower row contain the ionization potentials for the $Z+1$ atom. Column 7 contains the sums of these ionization potentials. Column 8 shows the calculated sum of ionization potentials for the $2p_{3/2}$-ionized atom (instead of the $Z+1$ ion). Column 9 shows the calculated correction to the $Z+1$ approximation for this quantity. Column 10 contains the resulting $2p_{3/2}$ binding energies. In columns 11 and 12 these energies are compared with available experiments.

1 Atom	2 I_1	3 I_2	4 I_3	5 I_4	6 I_5	7 ΣI_n	8 $(\Sigma I_n)^*$	9 7–8	10 E_c^{calc}	11 E_c^{expt}	12 $E_c^{calc}-E_c^{expt}$
Na	5.139	47.287				54.426			38.12	38.09[a]	0.03
	(Mg)	15.035				15.035	14.307	0.728			
Mg	7.646	15.035	80.145			102.826			57.64	57.54[b]	0.10
	(Al)	18.828	28.448			47.276	45.184	2.092			
Al	5.986	18.828	28.448	119.99		173.25			81.82		
	(Si)	16.346	33.493	45.142		94.981	91.430	3.551			
Si	8.152	16.346	33.493	45.142	166.77	269.90			108.91		
	(P)	19.726	30.18	51.368	65.025	166.30	160.99	5.31			

[a]Weighted average (see Ref. 162). [b]Reference 161.

With this value of α we then calculate the energy for the reaction $Mg^+(2p_{3/2}^3 s^2) \rightarrow Mg^{3+}(2p_{3/2}^3)$, and find 45.184 eV. Since the sum of the first three ionization potentials in magnesium is 102.826 eV, we obtain directly from Eqs. (A2) that the $p_{3/2}$ core ionization for the Mg atom is equal to $102.826 - 45.184 \simeq 57.64$ eV. This value should be compared with the experimental value of 57.57(10) eV obtained from Auger electron spectroscopy[38] and the value of 57.54 eV found from photoabsorption.[161] Thus, the agreement between our calculated value and experiment is good.

For the $2p_{3/2}$ core ionization in the aluminum atom we add together the first four ionization potentials, i.e., we obtain the energy for the process $Al(3s^2 3p) \rightarrow Al^{4+}(2p_{3/2}^3)$. This is 173.25 eV. Then we calculate the energy for the reaction $Si^+(3s^2 3p) \rightarrow Si^{4+}$ and vary α until the experimental value of 94.981 eV is obtained. With this value of α the energy of the step $Al^+(2p_{3/2}^3 3s^2 3p) \rightarrow Al^{4+}(2p_{3/2}^3)$ is computed to be 91.430 eV. From this we derive a (decoupled) $p_{3/2}$ core-ionization energy of 81.82 eV.

From these two examples the general procedure of the method should be rather obvious. In Table II we present our calculations for the $p_{3/2}$ core ionization for Na, Mg, Al, and Si, and show the experimental values we have used for the various ionization potentials. Measurements of the $p_{3/2}$ core ionization are available for sodium[58] and magnesium,[161] and as can be seen from Table II, the agreement is satisfactory. Therefore, one should also expect that the calculated values for aluminum and silicon should be rather accurate. However, quite naturally, the higher the ionization stage has to be before we arrive at the $2p_{3/2}^3$ configuration, the less accurate the derived values will be. This can be seen from column 9 in Table II, where the difference between the sum of valence ionization energies for the $(Z+1)$ substitution (ΣI_n) and the corresponding ionization energy for the Z atom with a core hole $[(\Sigma I_n)^*]$ is listed. In the case of silicon this difference attains quite a large value.

The same procedure as above, can be applied for the $3p_{3/2}$ core-electron ionization for the earlier elements in the fourth period, K–Cr. For elements beyond chromium some of the higher ionization potentials are no longer accurately known, which renders the present method inapplicable. In Table III we give the experimental and calculated data for K–Cr. In some cases, when we compare the appropriate valence electron ionization for the Z atom (with a core hole) and the $(Z+1)$ atom, we cannot directly use the ionization potentials, but have to correct for a configuration difference. Such a case is $Ca^+(3p_{3/2}^3 4s^2) \rightarrow Ca^{3+}(3p_{3/2}^3)$, where the ground state for the $(Z+1)$ ion, Sc^+, is $3d4s$. Thus the second ionization potential of scandium has to be subtracted by the excitation energy Sc II$(ds \rightarrow s^2)$. From Table III we note the good agreement between the computed values and the experimental values for potassium[58] and calcium.[163] It should also be noted that some of the ionization energies used in the calculation for vanadium and chromium might be somewhat erroneous. This, in addition to the large "correction" term in column 11, limits the accuracy of the derived core-ionization energies.

In Table IV we present the corresponding data for the earlier elements in the fifth period, Rb–Zr. Unfortunately, the present lack of accurate ionization energies does not permit reliable calculations for elements beyond zirconium. From the table we note the satisfying agreement between the calculated and measured value for the $4p_{3/2}$ electron ionization in rubidium[58] and

TABLE III. The $3p_{3/2}$ binding energies for the elements K–Cr, calculated with the method based on ionization potentials (method A). For a description of the columns see Table II.

1 Atom	2 I_1	3 I_2	4 I_3	5 I_4	6 I_5	7 I_6	8 I_7	9 ΣI_n	10 $(\Sigma I_n)^*$	11 9–10	12 E_c^{calc}	13 E_c^{expt}	14 $E_c^{calc} - E_c^{expt}$
K	4.341	31.625						35.966			24.61	24.57[a]	0.04
	(Ca)	11.872						11.872	11.357	0.515			
Ca	6.113	11.872	50.913					68.898			34.33	34.31[g]	0.02
	(Sc)	11.34[b]	24.757					36.10	34.57	1.53			
Sc	6.54	12.80	24.757	73.490				117.587			39.73		
	(Ti)	10.48[c]	27.492	43.267				81.23	77.86	3.37			
Ti	6.82	13.57	27.492	43.267	99.26			190.41			44.94		
	(V)	10.23[d]	29.310	46.709	65.281			151.53	145.47	6.06			
V	6.74	14.65	29.310	46.709	65.281	128.2		290.9			50.4		
	(Cr)	9.92[e]	30.96	49.1	69.5[f]	90.56		250.0	240.5	9.5			
Cr	6.766	16.50	30.96	49.1	69.5[f]	90.56	160.2	423.6			49.8		
	(Mn)	15.640	33.667	51.4[f]	72.3[f]	95.5[f]	119.27	387.8	373.8	14.0			

[a] Weighted average (see Ref. 162).
[b] Ionization from $Sc^+(s^2)$ which lies 1.455 eV above $Sc^+(ds)$.
[c] Ionization from $Ti^+(ds^2)$ which lies 3.095 eV above $Ti^+(d^2s)$.
[d] Ionization from $V^+(d^2s^2)$ which lies 4.42 eV (estimated value) above $V^+(d^4)$.
[e] Ionization from $Cr^+(d^3s^2)$ which lies 6.578 eV above $Cr^+(d^5)$.
[f] Estimated values from regularities of the $d^ns \rightarrow d^n$ ionization energies for +3, +4, and +5 ions.
[g] Reference 163.

TABLE IV. The $4p_{3/2}$ binding energies for the elements Rb–Zr, calculated with the method based on ionization potentials (method A). For a description of the columns see Table II.

1 Atom	2 I_1	3 I_2	4 I_3	5 I_4	6 I_5	7 ΣI_n	8 $(\Sigma I_n)^*$	9 7–8	10 E_c^{calc}	11 E_c^{expt}	12 $E_c^{calc}-E_c^{expt}$
Rb	4.177	27.285				31.462			20.86	20.87[a]	−0.01
	(Sr)	11.030				11.030	10.606	0.424			
Sr	5.695	11.030	42.87			59.59			28.00	28.21[e]	−0.21
	(Y)	12.23	20.525			32.75	31.59	1.16			
Y	6.38	12.23	20.525	60.60		99.74			33.53		
	(Zr)	11.36[b]	22.99	34.412		68.76	66.21	2.55			
Zr	6.84	13.13	22.99	34.412	80.35	157.72			37.7		
	(Nb)	11.32[c]	25.04	37.6[d]	50.55	124.5	120.0	4.5			

[a] Weighted average (see Ref. 162).
[b] Ionization from $Zr^+(ds^2)$ which lies 1.773 eV above $Zr^+(d^2s)$.
[c] Ionization from $Nb^+(d^2s^2)$ which lies 3.0 eV above $Nb^+(d^4)$. This value, 3.0 eV, has been estimated by the present authors.
[d] Estimated from regularities in the $d^ns \rightarrow d^n$ ionization energies for the +3 ions.
[e] Reference 39.

strontium.[39] Table V contains the pertinent information for the earlier elements in the sixth period, Cs–La. The literature value for the second ionization in Cs is 25.1 eV. However, a simple interpolation between the $5p$ ionizations in Xe, Ba^{2+}, and La^{3+} shows that a much more appropriate value should be 23.15(10) eV. This is supported by our present calculation for the $5p_{3/2}$ core ionization, which, after this replacement, agrees rather satisfactorily with the experimental value[58] (Table V). The computed $5p_{3/2}$ ionization energy for the barium atom is in excellent agreement with experiment.[23] For lanthanum, which has the atomic configuration ds^2, we need the energy position of the Ce II(ds^2) level. This level has not yet been identified in the Ce II spectrum, but its position can be estimated to be about 3.05(10) eV above the lowest d^3 level. This level in its turn is situated 4.03 eV above the ground state Ce II($4f5d^2$).

For the metals beyond the noble metals, the outermost d electrons behave essentially like core electrons. It is, therefore, possible to include these levels into our consideration of core-level binding-energy shifts. The method above can also be applied here to give sufficiently accurate estimates for some elements for which atomic core-ionization data otherwise are missing. The procedure is exactly the same as above, only that here in the last ionization process we ionize a $d_{5/2}$ electron. In Table VI the experimental ionization energies and our calculated values are given[164] for the elements Cu–Ga. Accurate values of the d-electron ionization in Cu and Zn can be obtained from the spectroscopic levels in Cu II and Zn II. Our calculated values compare favorably with these data. In the case of Ga the fourth ionization potential is not known, and therefore, the present method can not be directly applied in the form described above. In-

TABLE V. The $5p_{3/2}$ binding energies for the elements Cs–La, calculated with the method based on ionization potentials (method A). For a description of the columns see Table II.

1 Atom	2 I_1	3 I_2	4 I_3	5 I_4	6 ΣI_n	7 $(\Sigma I_n)^*$	8 6–7	9 E_c^{calc}	10 E_c^{expt}	11 $E_c^{calc}-E_c^{expt}$
Cs	3.894	23.15(10)[b]			27.05(10)			17.43(10)	17.37[a]	0.06(10)
	(Ba)	10.004			10.004	9.621	0.383			
Ba	5.2117	10.004	35.844		51.060			22.72	22.74[e]	−0.02
	(La)	10.143[c]	19.177		29.320	28.337	0.983			
La	5.5770	11.060	19.177	49.95(6)	85.76(6)			27.25(20)		
	(Ce)	3.77(10)[d]	20.198	36.758	60.72(10)	58.51	2.21			

[a] Weighted average (see Ref. 162).
[b] Estimated by the present authors (see text).
[c] Ionization from $La^+(s^2)$ which lies 0.917 eV above $La^+(d^2)$.
[d] Ionization from $Ce^+(ds^2)$ which lies 7.08(10) eV above $Ce^+(fd^2)$ (also see text).
[e] Reference 23.

TABLE VI. The $3d_{5/2}$ binding energies for the elements Cu–Ge, calculated with the method based on ionization potentials (method A). Columns 1–4 contain in the upper row the relevant ionization potentials for the Z atom and in the lower row contain the ionization potentials for the $Z+1$ atom. Column 6 shows the reaction used to create the $3d_{5/2}$ hole in those cases where not all valence electrons are stripped off the atom. Column 7 shows the energy for this excitation. Column 8 contains the sums of these ionization potentials (and excitation energies). Column 9 shows the calculated sum of ionization potentials for the $3d_{5/2}$-ionized atom (instead of the $Z+1$ ion). Column 10 shows the calculated correction to the $Z+1$ approximation for this quantity. Column 11 contains the resulting $3d_{5/2}$ binding energies. In column 12 and 13 these energies are compared to experiment wherever possible.

1 Atom	2 I_1	3 I_2	4 I_3	5 I_4	6 Excitation	7 E_{exc}	8 ΣI_n	9 $(\Sigma I_n)^*$	10 8–9	11 E_c^{calc}	12 E_c^{expt}	13 $E_c^{calc}-E_c^{expt}$
Cu	7.726	20.292					28.018			10.59	10.53[a]	0.06
	(Zn)	17.965					17.965	17.43	0.53			
Zn	9.394	17.965	39.722				67.081			17.28	17.17[c]	0.11
	(Ga)	20.51	30.71				51.22	49.80	1.42			
Ga	5.999	20.51			$d^{10}s \rightarrow d^9s^2$	16.16[b]	42.67			26.99		
	(Ge)	15.935					15.935	15.68	0.25			
Ge	7.899	15.935	34.224	45.713	$d^{10} \rightarrow d^9s$	29.19[a]	132.96			37.86		
	(As)	18.633	28.352	50.136			97.121	95.10	2.02			

[a] Weighted average (see Ref. 162).

[b] Estimated by the authors.

[c] Combination of Refs. 58 and 60.

TABLE VII. The $4d_{5/2}$ binding energies for the elements Ag–Sn, calculated with the method based on ionization potentials (method A). For a description of the columns see Table VI.

1 Atom	2 I_1	3 I_2	4 I_3	5 Excitation	6 E_{exc}	7 ΣI_n	8 $(\Sigma I_n)^*$	9 7–8	10 E_c^{calc}	11 E_c^{expt}	12 $E_c^{calc}-E_c^{expt}$
Ag	7.576	21.49				29.07			12.60	12.56[a]	0.04
	(Cd)	16.908				16.908	16.468	0.440			
Cd	8.994	16.908	37.48			63.38			17.65	17.58[b]	0.07
	(In)	18.870	28.03			46.90	45.73	1.17			
In	5.786	18.870		$d^{10}s \rightarrow d^9s^2$	14.329	38.985			24.61		
	(Sn)	14.632				14.632	14.375	0.257			
Sn	7.344	14.632	30.503	$d^{10}s \rightarrow d^9s^2$	20.982	73.461			32.4		
	(Sb)	16.53	25.3			41.8	41.1	0.7			

[a]Weighted average (see Ref. 162).

[b]Combination of Refs. 58 and 60.

stead, we can utilize the d^9s^2 level in Ga III. Consider the following reactions:

$$\mathrm{Ga}(d^{10}s^2p) \rightarrow \mathrm{Ga}^{2+}(d^9s^2), \quad \text{(A3a)}$$

$$\mathrm{Ga}^{+}(d^9s^2p) \rightarrow \mathrm{Ga}^{2+}(d^9s^2). \quad \text{(A3b)}$$

If both these reaction energies are known, we can directly obtain the $d_{5/2}$ core-electron ionization energy. The last process, Eq. (A2b), is compared with $\mathrm{Ge}^{+}(d^{10}s^2p) \rightarrow \mathrm{Ge}^{2+}(d^{10}s^2)$. From atomic calculations and α-fitting, we then calculate the (decoupled) excitation energy in Eq. (A2b) in the same way as before. For the accuracy of the result, it is a great advantage that we can utilize the Ga III(d^9s^2) level, since, in this way, the number of necessary ionization stages remains low. This is reflected by the small correction term, column 10 in Table VI. Unfortunately, the Ga III(d^9s^2) level has not been investigated experimentally, but its position above the Ga III$(d^{10}s)$ ground state can be estimated with a high accuracy. The same procedure has been used for Ge, where we utilized the Ge IV(d^9s^2) level.

Calculated and experimental values are shown for Ag–Sn in Table VII. For indium and tin the same method was used as above for gallium and germanium, respectively. The experimental d-ionization energies for atomic Ag and Cd agree very well with our calculated values. Table VIII gives the appropriate ionization potentials and calculated values for Au–Pb. Here the literature value of 34.2 eV[60] for the third ionization potential in mercury is somewhat uncertain. This can indeed, also be seen from the rather large discrepancy between our calculated value for the atomic d ionization and the experimental value. In view of the very good agreement for the corresponding ionization in Zn and Cd, a comparable accuracy should be expected for Hg. This suggests that a more proper value for the third ionization potential in Hg should be 34.7 eV. This modified value is also supported by the regularity of the ionization energies, $d^ns \rightarrow d^n$, for the +3 ions in the $5d$ series.

Above, we have shown that quite accurate core-electron ionization energies can be derived from other independent spectroscopic data, provided these data are supplemented by some simple atomic calculations. However, the somewhat limited accessibility of accurate experimental ionization potentials prevents a more extensive

TABLE VIII. The $5d_{5/2}$ binding energies for the elements Au–Pb, calculated with the method based on ionization potentials (method A). For a description of the columns see Table VI. For mercury, the values given within parentheses are discussed in the text.

1 Atom	2 I_1	3 I_2	4 I_3	5 Excitation	6 E_{exc}	7 ΣI_n	8 $(\Sigma I_n)^*$	9 7–8	10 E_c^{calc}	11 E_c^{expt}	12 $E_c^{calc}-E_c^{expt}$
Au	9.226	20.5				29.7			11.3	11.24[a]	0.06(10)
	(Hg)	18.756				18.756	18.353	0.403			
Hg	10.438	18.756	(34.2)			(63.4)			(14.4)	14.84[b]	(–0.4)
	(Tl)	20.428	29.852			50.280	48.976	1.304			
Tl	6.108	20.428		$d^{10}s \rightarrow d^9s^2$	8.290	34.826			20.09		
	(Pb)	15.032				15.032	14.737	0.295			
Pb	7.417	15.032	31.938	$d^{10}s \rightarrow d^9s^2$	12.554	66.941			25.49		
	(Bi)	16.69	25.56			42.25	41.45	0.80			

[a]Weighted average (see Ref. 162).

[b]Combination of Refs. 58 and 60.

TABLE IX. Summary of experimentally determined atomic binding energies which are used as starting points for the interpolation of $3d_{5/2}$ and $4f_{7/2}$ binding energies. The third column displays the values of the exchange parameter α which are found to reproduce these binding energies.

Core level	Energy [a] (eV)	α
Zn $3d_{5/2}$	17.168	0.7109
Kr $3d_{5/2}$	93.82(3)	0.7176
Sr $3d_{5/2}$	142.3(2)	0.7191
Cd $3d_{5/2}$	412.0(2)	0.7295
Xe $3d_{5/2}$	676.70(8)	0.7389
Yb $4f_{7/2}$	8.910	0.6947
Hg $4f_{7/2}$	107.06(5)	0.7188

[a] See Refs. 165 and 166.

use of this method. It should, for example, have been of special interest to apply this scheme to lutetium and hafnium, since for these elements the atomic $4f$ ionization energy could then have been derived. Unfortunately, one (or several) of the experimental ionization potentials in hafnium is likely to be quite erroneous, preventing the applicability of our scheme. The main restriction of the method is, however, the fact that only the outermost level of the core can be treated. In the next section of this Appendix, we present another approximative method which does not have this limitation.

2. Interpolation method

Since experimental data for core-electron binding energies are available for some elements, it seems reasonable to expect that some kind of interpolation between these values should give acceptable data for the intervening ele-

TABLE X. Experimental and interpolated $3d_{5/2}$ binding energies for the elements Zn–Xe. The second column shows the elements which have been used for the interpolation. The third column contains the calculated binding energies using a linear interpolation of the exchange parameter α between these elements. For comparison, the fourth column contains the binding energies calculated using a linearly interpolated value for the errors in a set of ΔSCF calculations. The fifth column contains the results from other calculations (method A) or experimentally determined binding energies which we, for various reasons, have chosen not to include in the interpolation procedure (see text).

Element	Interpolation	Energy (eV)	ΔSCF [a] (linearly corrected)	Other determinations
Zn		[17.168]	[17.168]	
Ga	Zn–Kr	27.03	27.11	26.99 (Calculated, method A)
Ge	Zn–Kr	38.05	38.34	37.86 (Calculated, method A)
As	Zn–Kr	50.35	50.64	
Se	Zn–Kr	63.77	63.87	
Br	Zn–Kr	78.27	78.32	
Kr		[93.82]	[93.82]	
Rb	Kr–Sr	117.24	117.31	117.33 [b] (Photoabsorption)
Sr		[142.3]	[142.3]	
Y	Sr–Cd	165.62	165.46	
Zr	Sr–Cd	189.53	189.25	
Nb	Sr–Cd	210.62	209.75	
Mo	Sr–Cd	235.86	235.01	
Tc	Sr–Cd	266.06	261.36 [c]	
Ru	Sr–Cd	289.03	288.24	
Rh	Sr–Cd	317.01	316.39	
Pd	Sr–Cd	341.55	340.61	
Ag	Sr–Cd	375.77	375.35	375.5 [d] (Auger)
Cd		[412.0]	[412.0]	
In	Cd–Xe	451.71	451.71	
Sn	Cd–Xe	493.10	493.50	
Sb	Cd–Xe	536.46	536.86	
Te	Cd–Xe	581.49	581.86	
I	Cd–Xe	628.25	628.45	
Xe		[676.70]	[676.70]	

[a] See Ref. 167.
[b] See Ref. 168.
[c] Calculated for the d^6s-configuration.
[d] See Ref. 72.

ments. Naturally, to get accurate results, it is desirable that the interpolation should be performed between elements close to each other in the periodic table. A particularly favorable case seems to be the $3d_{5/2}$ ionization, because here atomic data are available for Zn, Kr, Sr, Cd, and Xe.[165] For these elements we have calculated the $3d_{5/2}$ ionization energy and varied α until agreement with experiment was achieved. The values of α obtained in this manner are collected in Table IX. As a function of atomic number these α values display a regular and consistent behavior. The sensitivity of the calculated energy to a change of 0.001 in α is about 0.04 eV for zinc and 0.1 eV for xenon. This suggests that if a linear interpolation is made between the consecutive fitted α-values, appropriate ionization energies could be calculated for the intermediate elements. The values computed in this way are tabulated in Table X. The values for gallium and germanium can be compared with the previously derived values in Table VI. The agreement is gratifying.

The reason that we have not based any interpolation on the experimental Ag $3d_{5/2}$ ionization value[72] is that we expect the measurements of the Cd binding energies to be somewhat more accurate as concerns the absolute values. However, as can be seen from Table X a good agreement between the interpolated and the experimental Ag $3d_{5/2}$ binding energy is obtained.

The same method as above for the $3d_{5/2}$ level was also applied to the $4f_{7/2}$ ionization in the $5d$ series. Experimental atomic data are available only for ytterbium and mercury. The corresponding α values were derived and a linear interpolation was made, giving α values for the intermediate elements. From this, the $4f_{7/2}$ ionization energies for the $5d$ elements were calculated and the results are presented in Table XI. In this table we also include some calculated results for elements beyond mercury, obtained from linearly *extrapolated* α values.

For Tl, Pb, and Bi, we can compare the extrapolated $4f_{7/2}$ binding energies with experimentally determined values. As can be seen from Table XI they seem to differ by about 0.5 eV. It is, however, not quite clear which quantities are the most accurate ones for these elements, the extrapolated or the experimental ones. We can, however, obtain additional estimates of the atomic binding energies by combining the calculated ΔE_c shifts with the measured solid-phase binding energies. As was pointed out in Sec. VI, we expect the calculated ΔE_c shifts to be particularly accurate for the elements in this region of the sixth period. Since the estimated errors in the solid-phase binding energies are also quite small, we expect the obtained atomic $4f$ binding energies to be quite accurate.

TABLE XI. Experimental, interpolated, and extrapolated $4f_{7/2}$ binding energies for the elements Yb–Bi based on the experimentally known values for Yb and Hg. The second column contains the binding energies calculated using a linear interpolation or extrapolation for the exchange parameter α. For comparison, the third column contains the binding energies calculated using a linearly interpolated or extrapolated value for the errors in a set of ΔSCF calculations. The fourth column contains experimentally determined binding energies which we, for various reasons, have chosen not to include in the interpolation/extrapolation procedure (see text).

Element	Energy[a] (eV)	ΔSCF[b] (Linearly corrected)	Experimental
Yb	[8.910]	[8.910]	
Lu	15.89	16.44	
Hf	23.61	24.26	
Ta	31.96	32.74	
W	40.87	41.44	
Re	50.61	51.31	
Os	60.91	61.55	
Ir	71.66	65.94[c]	
Pt	79.86	79.82	
Au	91.52	91.20	
Hg	[107.06]	[107.06]	
Tl	125.19	125.13	125.75[d]
Pb	144.15	144.18	144.0[e], 143.6[f]
Bi	164.66	164.49	164.9[e]

[a] All α values are interpolated or extrapolated between Yb and Hg.
[b] See Ref. 169.
[c] Calculated for the d^9 configuration.
[d] See Ref. 26.
[e] See Ref. 20.
[f] See Ref. 28.

For Tl we have calculated the ΔE_c shift to be 7.60 eV. This value is also supported by the pseudoexperimental point based on the $5d_{5/2}$ level, (see Fig. 7). Combining this shift with the measured solid-phase binding energies[88] [122.17(10) eV and 117.73(10) eV], we obtain 129.8 and 125.3 eV for the $4f_{5/2}$ and $4f_{7/2}$ atomic binding energies, respectively. The atomic $4f_{7/2}$ binding energy obtained in this way thus agrees well with the extrapolated value in Table XI but not with the experimental energy. Therefore, it seems that the experimental atomic binding energies in Ref. 26 might be somewhat too high.

For Pb we have calculated the ΔE_c shift to be 7.44 eV. As for Tl, the calculated shift is supported by the pseudoexperimental $5d_{5/2}$ shift, (see Fig. 7). In this case we obtain, by combining the calculated ΔE_c value with the experimental

solid-phase binding energies,[88] [141.69(10) eV and 136.65(10) eV] as our estimates for the atomic $4f$ binding energies 149.1 and 144.1 eV for the $\frac{5}{2}$ and $\frac{7}{2}$ components, respectively. This value is also in good agreement with the one derived from photoelectron spectroscopy,[20] but in somewhat worse agreement with the experimental photoabsorption value.[28]

For Bi a good agreement is found between the calculated ΔE_c shift and the experimental $4f$ shift (Ref. 20 for the atomic and Ref. 88 for the solid-phase binding energies). Furthermore, from Table XI we can see that a fairly good agreement is obtained between the extrapolated and experimental $4f_{7/2}$ binding energies. A conclusion that can be drawn from the above comparisons between extrapolated and experimental binding energies is that the binding energies calculated in this way seem to be accurate to within a few tenths of an eV.

Finally, the same type of approach was used for the $6p_{3/2}$ ionization in thorium and uranium. Here, an adapted value of α was obtained from the known ionization energy[60] of radon (10.748 eV). With this fitted α value the corresponding $6p_{3/2}$ ionization energies for Th(d^2s^2) and U(d^4s^2) were calculated to be 25.8 and 31.3 eV, respectively.[170]

[1] K. Siegbahn, C. Nordling, G. Johansson, J. Hedman, P. F. Hedén, K. Hamrin, U. Gelius, T. Bergmark, L. O. Verme, R. Manne, and Y. Baer, *ESCA Applied to Free Molecules* (North-Holland, Amsterdam, 1969).

[2] *Topics in Applied Physics; Photoemission in Solids I, General Principles; Photoemission in Solids II, Case Studies*, edited by M. Cardona and L. Ley (Springer Verlag, Berlin, 1978), Vols. 26 and 27.

[3] *Structure and Bonding, Photoelectron Spectrometry*, edited by J. D. Dunitz, P. Hemmerich, R. H. Holm, J. A. Ibers, C. K. Jørgensen, J. B. Neilands, D. Reinen, and R. J. P. Williams (Springer Verlag, Berlin, 1975).

[4] L. Ley, S. P. Kowalczyk, F. R. McFeely, R. A. Pollak, and D. A. Shirley, Phys. Rev. B 8, 2392 (1973).

[5] R. E. Watson and M. L. Perlman, in Ref. 3, p. 83.

[6] R. E. Watson, M. L. Perlman, and J. F. Herbst, Phys. Rev. B 13, 2358 (1976).

[7] A. R. Williams and N. D. Lang, Phys. Rev. Lett. 40, 954 (1978).

[8] F. P. Larkins, J. Phys. C 10, 2461 (1977).

[9] D. A. Shirley, R. L. Martin, S. P. Kowalczyk, F. R. McFeely, and L. Ley, Phys. Rev. B 15, 544 (1977).

[10] R. Hoogewijs, L. Fiermans, and J. Vennik, Surf. Sci. 69, 273 (1977).

[11] P. Weightman, P. T. Andrews, and L. A. Hisscott, J. Phys. F 5, L220 (1975).

[12] J. F. Herbst, R. E. Watson, and J. W. Wilkins, Phys. Rev. B 13, 1439 (1976).

[13] J. F. Herbst, R. E. Watson, and J. W. Wilkins, Phys. Rev. B 17, 3089 (1978).

[14] R. Hoogewijs, L. Fiermans, and J. Vennik, Chem. Phys. Lett. 37, 87 (1976).

[15] D. R. Beck and C. A. Nickolaides, Int. J. Quantum Chem. Symp. 10, 119 (1976).

[16] J. Q. Broughton and D. L. Perry, J. Electron Spectrosc. Relat. Phenom. 16, 45 (1979).

[17] L. Hedin, Ark. Fys. 30, 231 (1965).

[18] P. H. Citrin and D. R. Hamann, Phys. Rev. B 10, 4948 (1974).

[19] S. Svensson, N. Mårtensson, E. Basilier, P. -Å. Malmqvist, U. Gelius, and K. Siegbahn, J. Electron Spectrosc. Relat. Phenom. 9, 51 (1976).

[20] Y. S. Khodeyev, H. Siegbahn, K. Hamrin, and K. Siegbahn, Chem. Phys. Lett. 19, 16 (1973).

[21] S. P. Kowalszyk, L. Ley, F. R. McFeely, R. A. Pollack, and D. A. Shirley, Phys. Rev. B 8, 3583 (1973).

[22] M. S. Banna, B. Wallbank, D. C. Frost, C. A. McDowell, and J. S. H. Q. Perera, J. Chem. Phys. 68, 5459 (1978).

[23] B. Breuckmann, Ph.D. thesis, University of Freiburg (unpublished).

[24] D. A. Shirley, R. L. Martin, B. E. Mills, S. Süzer, S. -T. Lee, E. Matthias, and R. A. Rosenberg, in *Proceedings of 2nd International Conference on Inner Shell Ionization Phenomena*—Invited Papers, 1976, Freiburg, West Germany, edited by W. Mehlhorn and R. Brenn (Universität Freiburg, Freiburg, Germany, 1976), p. 238.

[25] C. S. Fadley and D. A. Shirley, Phys. Rev. A 2, 1109 (1970).

[26] J. P. Connerade and M. W. D. Mansfield, Proc. R. Soc. London, Ser. A 344, 435 (1975).

[27] J. P. Connerade and M. W. D. Mansfield, Proc. R. Soc. London, Ser. A 335, 87 (1973).

[28] J. P. Connerade, B. Drerup, and M. W. D. Mansfield, Proc. R. Soc. London, Ser. A 348, 235 (1976).

[29] D. H. Tracy, Proc. R. Soc. London, Ser. A 357, 485 (1977).

[30] M. W. D. Mansfield and J. P. Connerade, Proc. R. Soc. London, Ser. A 344, 303 (1975).

[31] H. Petersen, K. Radler, B. Sonntag, and R. Haensel, J. Phys. B 8, 31 (1975).

[32] R. Bruhn, B. Sonntag, and H. W. Wolff, DESY Reports Nos. SR 78/14, 1978 and 78/16, 1978 (unpublished); J. Phys. B 12, 203 (1979).

[33] D. L. Ederer, T. B. Lucatorto, E. B. Saloman, R. P. Madden, and J. Sugar, J. Phys. B 8, L21 (1975).

[34] W. R. S. Garton, J. P. Connerade, M. W. D. Mansfield, and J. E. G. Weaton, Appl. Opt. 8, 919 (1969).

[35] S. Aksela, J. Väyrynen, and H. Aksela, Phys. Rev. Lett. 33, 999 (1974).

[36] J. Väyrynen, S. Aksela, and H. Aksela, Phys. Scr. 16, 452 (1977).

[37] H. Hillig, B. Cleff, W. Mehlhorn, and W. Schmitz, Z. Phys. 268, 225 (1974).

[38] B. Breuckmann, V. Schmidt, and W. Schmitz, J. Phys. B 9, 3037 (1976).

[39] W. Schmitz, B. Breuckmann, and W. Mehlhorn, J. Phys. B 9, L493 (1976).

[40]D. J. Pegg, H. H. Haselton, R. S. Thoe, P. M. Griffin, M. D. Brown, and I. A. Sellin, Phys. Rev. A 12, 1330 (1975).
[41]P. Ziem, R. Bruch, and N. Stolterfoht, J. Phys. B 8, L480 (1975).
[42]P. Bisgaard, R. Bruch, P. Dahl, B. Fastrup, and M. Rødbro, Phys. Scr. 17, 49 (1978); M. Rødbro, R. Bruch, and P. Bisgaard, J. Phys. B 12, 2413 (1979).
[43]N. Mårtensson and B. Johansson, Solid State Commun. 32, 791 (1979).
[44](a) J. C. Riviére, *Solid State Surface Science*, Vol. I, edited by M. Green (Dekker, New York, 1973). (b) In principle, the use of this relation requires a specification of the sample surface.
[45]J. Friedel, Philos. Mag. 43, 153 (1952).
[46]J. F. Herbst, D. N. Lowy, and R. E. Watson, Phys. Rev. B 6, 1913 (1972).
[47]This can be understood as follows: First imagine that we determine the position of the Fermi level by photoionization. The final state of this process corresponds to a hole at the Fermi level. Next imagine that we ionize a core electron from the system. The assumed total screening of the ionized site can be accomplished most favorably by an electron from the Fermi level. Therefore, the final state is an impurity site (totally screened) and a hole at the Fermi level. The difference between the two measurements then corresponds to the quantity $E^M_{c,F}$. The fact that the hole created in the second process is for a system with one impurity site makes a totally negligible difference.
[48]A. R. Miedema, J. Less-Common Met. 46, 67 (1976). In this semiempirical scheme, the energy effect on binary solid alloy formation is derived from a negative term from the difference in chemical potential, ϕ^*, for electrons at the two types of atomic cells, and a second term that reflects the discontinuity in the density of electrons, n_{WS}, at the boundary between dissimilar atomic cells. The parameters ϕ^* and n_{WS} are properties of the pure metals.
[49]This was observed for mercury by Svensson *et al.* (Ref. 19). In the case of cesium the same conclusion can be drawn from the data in Refs. 22, 31, and 50.
[50]G. Ebbinghaus Ph.D. thesis, Stuttgart, 1977 (unpublished).
[51]For several elements the $(Z+1)$ approximation has been found to reproduce atomic shake-up and shake-off energies with a high accuracy (Refs. 19, 22, 32, 52, and 53). For instance, in Ref. 22 good recordings of the shake-up satellites have been made for all alkali metal atoms except Li, and in all these cases the satellites could very well be reproduced by the $Z+1$ approximation. However, the comment made in Ref. 22 that the $Z+1$ approximation fails to reproduce the Mg shake-up energies, is based on a confusion of the shake-up concept in photoelectron and Auger spectra. For an initial state shake-up process in an Auger spectrum the extra electron-hole pair excitation will be present both in the initial and final state. An equivalent core analysis of the Auger satellite spectra will thus involve both the $Z+1$ and $Z+2$ approximations. The inclusion of the $Z+2$ approximation makes the errors somewhat larger but the satellite spectra can also here be reproduced to within a few eV. For the Mg photoelectron satellite spectrum it seems most plausible that the peak at 6.1 eV corresponds to a $3s$–$4p$ inelastic loss. The fact that the peak at 12.3 eV does not fit too well for the shake-up energy calculated from the $Z+1$ approximation (11.4 eV), might indicate that this peak also contains a considerable contribution from inelastic scattering. A further interpretation of this satellite spectrum should, therefore, require recordings made at a lower sample pressure.
[52]S. Svensson, N. Mårtensson, E. Basilier, P.-Å. Malmqvist, U. Gelius, and K. Siegbahn, Phys. Scr. 14, 141 (1976).
[53]U. Gelius, J. Electron Spectrosc. Relat. Phenom. 5, 985 (1974).
[54]N. Mårtensson and B. Johansson (unpublished).
[55]B. Johansson (unpublished).
[56]K. A. Gschneidner, Jr., Solid State Phys. 16, 275 (1964).
[57]L. Brewer, LBL Report No. LBL 3720 (unpublished).
[58]C. E. Moore, *Atomic Energy Levels*, U. S. Natl. Bur. Stand. Circ. No. 467 (U.S.) Vols. I–III (1958); *Atomic Energy Levels*, Nat. Stand. Ref. Data Ser., Nat. Bur. Stand. (U.S.), 35, Vol. I (1971).
[59]W. C. Martin, R. Zalubas and L. Hagan, *Atomic Energy Levels-The Rare-Earth Elements*, Nat. Bur. Stand. (U.S.) Spec. Publ. 60 (1978).
[60]C. E. Moore, *Ionization Potentials and Ionization Limits Derived from the Analyses of Optical Spectra*, Nat. Stand. Ref. Data Ser., Nat. Bur. Stand. (U.S.), 34 (1970).
[61]S. -E. Johansson (private communication).
[62]Most of the solid state data are taken from a recent tabulation in Ref. 2. Other references are: Petersson and Karlsson[63] (solid K); Mårtensson *et al.*[64] (solid Ca, Sr and Ba); Nyholm and Mårtensson[65] (solid Ag and Cd); Baer and Lang[66] (solid Yb); Svensson *et al.*[19] (atomic and solid Hg); Mårtensson *et al.*[67] (solid Tl and Pb); Baer[68] (solid Bi).
Most of the atomic data are from a recent tabulation in Ref. 69. Other references are: Pekeris[70] (atomic Li); Bispgaard *et al.*[42] (atomic Be); Banna *et al.*[22] (atomic Na, K, Rb, Cs, and Mg); Bruhn *et al.*[32] (atomic Cu); Banna *et al.*[71] (atomic Zn and Cd); Aksela[72] (atomic Ag); Peterson *et al.*[31] (atomic Cs); Tracy[29] (atomic Yb); Martin *et al.*[59] (atomic Yb); Connerade and Mansfield[26] (atomic Tl); Connerade *et al.*[28] (atomic Pb); Khodeyev *et al.*[20] (atomic Bi).
[63]L. -G. Petersson and S. -E. Karlsson, Phys. Scr. 16, 425 (1977).
[64]N. Mårtensson, L. Ley, and J. Azoulay (unpublished).
[65]R. Nyholm and N. Mårtensson, J. Phys. C, in press.
[66]Y. Baer and J. K. Lang (unpublished).
[67]N. Mårtensson, A. Berndtsson, and R. Nyholm (unpublished).
[68]Y. Baer, Commun. Phys. Lab. Univ. Leiden 2, 65 (1977).
[69]W. Mehlhorn, B. Breuckmann, and D. Hausamann, Phys. Scr. 16, 177 (1977).
[70]C. H. Pekeris, Phys. Rev. 126, 143 (1962).
[71]M. S. Banna, D. C. Frost, C. A. McDowell, and B. Wallbank, J. Chem. Phys. 68, 696 (1978).
[72]S. Aksela (private communication).
[73]Often when the main aim of an electron spectroscopic investigation is not directed towards accurate binding-energy measurements, the spectra might be insufficiently calibrated. Furthermore, there are still some ambiguities regarding the proper binding energies of

the commonly used calibration lines (e.g., Refs. 74–75). There might also be differences concerning the meaning of the binding energy of a certain level. An example of this is the case when an incompletely resolved spin orbit doublet is analyzed. Here one might, for instance, report the energy of the main component after a deconvolution, the energy of the dominant peak without a deconvolution or the center of gravity of the complete doublet. The peak position itself can also be defined in a variety of ways. This might lead to particularly large uncertainties if the lines are wide, asymmetric, or associated with a high background rise. A common way to calibrate electron spectra is to evaporate a film of gold on top of the sample. Some workers prefer to evaporate films which are so thin that the signals from the sample can be recorded simultaneously. This method might, however, be somewhat hazardous, e.g., because of island formation or alloying, and quite different values for the Au binding energies might be obtained (Ref. 139). Some of the free-atomic values are derived indirectly from Auger or photoabsorption measurements. In these cases, the obtained binding energies are dependent on the proper assignments of the final states. There might in some cases also be difficulties in the analysis due to multiplet-splitting effects.

[74]K. Asami, J. Electron Spectrosc. Relat. Phenom. 9, 469 (1976).

[75]H. Ågren, J. Nordgren, L. Selander, C. Nordling, and K. Siegbahn, J. Electron Spectrosc. Relat. Phenom. 14, 27 (1978).

[76]B. Johansson, Phys. Rev. B 19, 6615 (1979).

[77]The results in the following paragraph require that the atomic absorption involves the lowest unoccupied level of the core-ionized atom.

[78]For Sc we have used the recent data by J. K. Gimzewski, D. J. Fabian, L. M. Watson, and S. Affrossman, J. Phys. F 7, L305 (1977); otherwise data from Ref. 2 are utilized.

[79]K. Siegbahn, C. Nordling, A. Fahlman, R. Nordberg, K. Hamrin, J. Hedman, G. Johansson, T. Bergmark, S. -E. Karlsson, I. Lindgren, and B. Lindberg, Nova Acta Regiae Soc. Sci. Ups. 20 (1967), and U. Gelius and K. Siegbahn, Faraday Discuss. Chem. Soc. 54, 257 (1972).

[80]For chromium a value of 707 eV was calculated in Ref. 79, which should be compared with the more recent result, 704.21 eV (Ref. 81). The reason for this large discrepancy is that the chromium binding energies in Ref. 79 were obtained without making any final-state calculations. Instead, the atomic reorganization energies were obtained by a linear interpolation between V and Mn. Thus the smooth trend for the reorganization energies which is observed for the other elements in the $3d$ series does not hold for chromium, which is most likely due to its d^5s atomic configuration.

[81]K. N. Huang, M. Aoyagi, M. H. Chen, B. Crasemann, and H. Mark, At. Data 18, 243 (1976).

[82]The Zn $2s$ atomic binding energy is obtained by combining the $2p_{3/2}$ atomic binding energy from Ref. 71 with the $2s-2p_{3/2}$ binding energy difference for the solid obtained from Ref. 9. Note that the $2s$ binding energy in Ref. 2 is quoted wrongly by about 4.5 eV.

[83]The decision to use the $2s$ level turns out to be somewhat unfortunate. First of all, for this level the inherent width is of the order of 5 eV. Furthermore, due to low signal-to-background ratios and high background contributions from the lines themselves, the peak positions are difficult to determine (see also Ref. 73). In fact, a reinvestigation of some of the $2s$ binding energies in this series shows that the error limits quoted in Ref. 9 are far too small (N. Mårtensson, A. Berndtsson, and R. Nyholm, unpublished).

[84]Here valence is used to denote the number of s electrons. Later, when we treat the lanthanides, the valence concept stands for the total number of d and s electrons. When Yb and Lu are treated together with the $5d$ elements, we again let valence be synonymous with the number of s electrons. Thus valence is used just as a short and convenient notation for the atomic configuration.

[85]For Y the solid state data given in Ref. 2 are used. For Zr–Sn we have employed data from Ref. 65.

[86]For the metallic binding energies we have used Ref. 2 for La and Au. Other references are: Baer and Lang[66] (solid Lu); Steiner *et al.*[87] (solid Hf); Berndtsson *et al.*[88] (solid Ta, W, Ir, and Pt); Berndtsson *et al.*[89(a)] (solid Re and Os).

[87]P. Steiner, H. Höchst, J. Schneider, S. Hüfner, and C. Politis, Z. Phys. 33, 241 (1979).

[88]A. Berndtsson, R. Nyholm, and N. Mårtensson (unpublished).

[89](a) A. Berndtsson, R. Nyholm, N. Mårtensson, R. Nilsson, and J. Hedman, Phys. Status Solidi B 93, K103 (1979). (b) We have used the calculated Pb $5d_{5/2}$ binding energy instead of the experimental value from Ref. 69, since in this way we can avoid the problems associated with the multiplet splitting of the $5d^96s^26p^2$ configuration. Note, however, that the experimental binding energy quoted in Ref. 69 is 25.28 eV, i.e., only 0.2 eV from our calculated value.

[90]K. A. Gschneidner, Jr., *Rare Earth Alloys* (Van Nostrand, Princeton, N. J., 1961).

[91]B. Johansson and A. Rosengren, Phys. Rev. B 11, 2836 (1975).

[92]For those rare-earths which have the same occupation of the f shell in the atom as in the metal, the "core-hole"-f^n multiplet splitting will be practically identical in the atom and the solid. Therefore, for these elements the derived ΔE_c shift will be the same for each level of the multiplet. However, for the atom there is an additional complication due to the $5d$ electron. This d electron gives rise to further splitting, but the influence of this on the experimental ΔE_c shift will still be quite small.

For the other lanthanides there will be a "core-hole"-f^{n+1} multiplet splitting for the atom but a "core-hole"-f^n splitting in the metal. For deep core holes this difference in multiplets will be almost negligible. For less deep core holes it will give rise to some additional structure to the calculated smooth behavior of ΔE_c through the series.

In this connection it is of interest to compare with the $4d$ photoabsorption spectra of the lanthanides. These spectra are dominated by a $4d^{10}4f^n \rightarrow 4d^94f^{n+1}$ transition. For La,[a] Ce,[b] and Eu[c] there is an excellent agreement between the spectra in the vapor and the solid phase, and in particular there is no wavelength shift. This is similar to our statement above, con-

cerning the identical energy shift ΔE_c for the various multiplet levels of the "core-hole"-f^n configuration for those lanthanides which attain the same valence state in the atom and the solid. The elements just mentioned belong to this category. Radtke[d] has also demonstrated that the structure in the 4*d* photoabsorption spectrum of a divalent lanthanide Z atom is almost identical to that for the $(Z+1)$ metal, provided this metal is trivalent. However, there is, of course, a wavelength shift. In the same way, one would expect that the multiplet splitting of the final state of a core-ionized divalent Z atom will be similar to that in the $(Z+1)$ metal, although somewhat displaced in energy.

[a]E. -R. Radtke, J. Phys. B 12, L71 (1979).
[b]H. -W. Wolff, R. Bruhn, K. Radler, and B. Sonntag, Phys. Lett. A 59, 67 (1976).
[c]M. W. D. Mansfield and J. P. Connerade, Proc. R. Soc. London, Ser. A 352, 125 (1976).
[d]E. -R. Radtke, J. Phys. B 12, L77 (1979).

[93]In the derived ΔE_c shifts we have neglected the difference between the Racah parameters for the f^n configuration of the Z atom and the f^n configuration of the $(Z+1)$ atom. This approximation is certainly appropriate in the present context since the error made is usually smaller than 0.2 eV. Only in the middle of the series are somewhat larger errors found[76].

[94]Actually, aluminum metal has not been treated in the previous sections. For the free atom we calculate the $2p_{3/2}$ ionization energy to be 81.82 eV (see Appendix). For the metal the $2p_{3/2}$ binding energy relative to the Fermi level has been measured[95] to be 72.5(2) eV. Thus the pseudoexperimental value for the shift is 9.3(2) eV. Our calculated ΔE_c shift is 9.13 eV, showing a good agreement with experiment. It should be noted that in our calculation the (hypothetical) metallic cohesive energy for the $(Z+1)$ element, Si, has been used. This has been estimated[48] to be 4.28(10) eV.

[95]P. H. Citrin, G. K. Wertheim, and Y. Baer, Phys. Rev. B 16, 4256 (1977).
[96]F. L. Oetting, M. H. Rand, and R. J. Ackermann, *The Chemical Thermodynamics of Actinide Elements and Compounds, Part 1 The Actinide Elements* (International Atomic Energy Agency, Vienna, 1976).
[97]L. Brewer, J. Opt. Soc. Am. 61, 1101 (1971); 61, 1682 (1971).
[98]W. C. Martin, L. Hagan, J. Reader, and J. Sugar, J. Phys. Chem. Ref. Data 3, 771 (1974).
[99]J. Sugar, J. Chem. Phys. 60, 4103 (1974).
[100]R. W. Solarz, C. A. May, L. R. Carlson, E. F. Worden, S. A. Johnson, J. A. Paisner, and L. J. Radziemski, Phys. Rev. A 14, 1129 (1976).
[101]L. J. Nugent, J. L. Burnett, and L. R. Morss, J. Chem. Thermodyn. 5, 665 (1973).
[102]B. Johansson and A. Rosengren, Phys. Rev. B 11, 1367 (1975).
[103]J. W. Ward, P. D. Kleinschmidt, and R. G. Haire, J. Phys. (Paris) Colloq. 4, 233 (1979).

[104]Actually this has not yet been demonstrated experimentally. However, the fact that Cf is very close to being divalent[105,106] means that, due to the increased binding energy of the f electrons, the heavier actinides are very likely to be divalent metals.

[105]M. Noé and J. R. Peterson, in *Transplutonium Elements*, edited by W. Müller and R. Lindner (North-Holland, Amsterdam, 1976), p. 69.
[106]B. Johansson, Phys. Rev. B 19, 6615 (1979).
[107]*The Actinides; Electronic Structure and Related Properties*, edited by A. J. Freeman and J. B. Darby, Jr. (Academic, New York, 1974), Vols. I and II.
[108]*Proceedings 2nd International Conference On the Electronic Structure of the Actinides*, edited by J. Mulak, W. Suski, and R. Troć (Ossolineum, 1977).
[109]J. Phys. (Paris) Colloq. 4 (1979).
[110]W. H. Zachariasen, Acta Crystallogr. 5, 660 (1952).
[111]W. H. Zachariasen, J. Inorg. Nucl. Chem. 35, 3487 (1973).
[112]M. B. Brodsky, Rep. Prog. Phys. 41, 1547 (1978).

[113]Most of the data are obtained from Ref. 2. Other references are: Petersson and Karlsson[63] (K3p); Mårtensson *et al.*[64] (Ca3p, Sr4$p_{3/2}$, and Ba5$p_{3/2}$); Gimzewski *et al.*[78] (Sc3p); Nyholm *et al.*[65] (Zr4$p_{3/2}$, Nb4$p_{3/2}$, Mo4$p_{3/2}$ Ru4$p_{3/2}$ and Rh4$p_{3/2}$); Berndtsson *et al.*[88] (Ta5$p_{3/2}$, W5$p_{3/2}$, and Ir5$p_{3/2}$); Berndtsson *et al.*[89] (Os5$p_{3/2}$); Fuggle *et al.*[114] (Th6$p_{3/2}$ and U6$p_{3/2}$).

[114]J. C. Fuggle, A. F. Burr, L. M. Watson, D. J. Fabian, and W. Lang, J. Phys. F 4, 335 (1974).
[115]E. A. Kmetko and H. H. Hill, *Plutonium 70*, edited by W. N. Miner, (AIME, New York, 1970), p. 233.
[116]H. H. Hill, *Plutonium 70*, edited by W. N. Miner (AIME, New York, 1970), p. 2.
[117]A. J. Freeman and D. D. Koelling, Ref. 107, Vol. I, p. 51.
[118]B. Johansson, Phys. Rev. B 11, 2740 (1975); and B. Johansson, Inst. Phys. Conf. Ser. No. 37, 39 (1978).
[119]J. F. Herbst, R. E. Watson, and I. Lindgren, Phys. Rev. B 14, 3265 (1976).
[120]A. J. Freeman, Inst. Phys. Conf. Ser. No. 37, 120 (1978).
[121]H. L. Skriver, O. K. Andersen, and B. Johansson, Phys. Rev. Lett. 41, 42 (1978).
[122]H. L. Skriver, O. K. Andersen, and B. Johansson (unpublished).
[123]P. H. Citrin, G. K. Wertheim, and Y. Baer, Phys. Rev. Lett. 41, 1425 (1978).
[124]G. K. Wertheim, J. H. Wernick, and G. Creselius, Phys. Rev. B 18, 875 (1978).
[125]Tran Minh Duc, C. Guillot, Y. Lassailly, J. Lecante, Y. Jugnet, and J. C. Vedrine, Phys. Rev. Lett. 43, 789 (1979).

[126]With surface cohesive energy we mean the energy gained when a free atom is brought to the metal surface while enlarging the surface area.

[127]The surface impurity term refers to a $(Z+1)$ surface atom [on the $(Z+1)$ metal] dissolved at the surface of the Z metal.

[128]B. C. Allen, in *Liquid Metals Chemistry and Physics*, edited by S. Z. Beer (Dekker, New York, 1972), p. 161.
[129]A. A. Lucas, in *Collective Properties of Physical Systems*, edited by B. Lundqvist, S. Lundqvist, and V. Runnström-Reio (Academic, New York, 1973), p. 169.
[130]A. S. Skapski, J. Chem. Phys. 16, 389 (1948).
[131]A. S. Skapski, Acta Metall. 4, 576 (1956).
[132]R. Evans, J. Phys. C 7, 2808 (1974).
[133]S. F. Alvarado, M. Campagna, and W. Gudat, J. Electron Spectrosc. Relat. Phenom. 18, 43 (1980).

[134]What supports the surface contamination interpretation in Ref. 133 is the presence of some structures in the photoelectron spectrum at 7.5 and 12 eV from the Fermi level. The latter structure has, in previous investigations been associated with surface contaminants.[a,b]

However, these features alone do not prove the validity of this interpretation. On the other hand, what supports the present view, i.e., that of a shifted surface component as an inherent property of the Yb surface, is the fact that the intensity ratio between the two shifted components was found to be constant, irrespective of whether the sample was prepared by mechanical scraping (performed at 2×10^{-10} Torr) or by evaporation. Furthermore, the intensity ratio was found to remain constant over several hours in the spectrometer. The strong intensity of the shifted $4f$ components also indicates that there should be almost a monolayer of the contaminants at the surface. Since the contaminants are likely to be dominated by oxygen, this would imply a surface compound of YbO. However, it is quite likely that such a surface is unstable and has to contain a considerable amount of the trivalent ytterbium oxide, Yb_2O_3. Since the authors of Ref. 133 explicitly state that they see no trace of trivalent Yb in their spectra, we tend to believe that the observed surface shift could not originate from oxygen contamination. A possible interpretation of the 7.5 and 12 eV structures could then be that these are due to shake-up processes leading to two-hole final states in the f shell. Resonance type of experiments could clarify the situation.

[a]W. C. Lang, B. D. Padalia, D. J. Fabian, and L. M. Watson, J. Electron Spectrosc. Relat. Phenom. 5, 207 (1974).

[b]G. Brodén, S. B. M. Hagström, and C. Norris, Phys. Rev. Lett. 24, 1173 (1970).

[135]G. K. Wertheim and G. Crecelius, Phys. Rev. Lett. 40, 813 (1978).

[136]J. W. Allen, L. I. Johansson, R. S. Bauer, I. Lindau, and S. B. M. Hagström, Phys. Rev. Lett. 41, 1499 (1978).

[137]J. K. Lang and Y. Baer, Solid State Commun. (to be published).

[138]A compilation of the binding energies in Ne, Ar, and Kr has been made by Johansson *et al.*[139] More recent data can be found in Ågren *et al.*[75] (Ne 1s); Nordgren *et al.*[140] (Ar 2s and 2p); Svensson *et al.*[52] (Xe 3s, 3p, 3d, 4s, 4p, 4d, and 5s). New values for Kr $3d_{3/2,5/2}$ can be obtained from a recent $M_{4,5}NN$ Auger spectrum (Ohtani *et al.*[141]). In this work one obtained Auger energies which were consistently 0.20 ± 0.03 eV higher than previous values. This discrepancy was resolved by Hansen and Persson[142] who could attribute this to an error of 0.20 eV in the second ionization potential of Kr.[143]

[139]G. Johansson, J. Hedman, A. Berndtsson, M. Klasson, and R. Nilsson, J. Electron Spectrosc. Relat. Phenom. 2, 295 (1973).

[140]J. Nordgren, H. Ågren, C. Nordling, and K. Siegbahn, Phys. Scr. 19, 5 (1979).

[141]S. Ohtani, H. Nishimura, H. Suzuki, and K. Wakiya, Phys. Rev. Lett. 36, 863 (1976).

[142]J. E. Hansen and W. Persson, Phys. Rev. A 20, 364 (1979).

[143]L. Minnhagen, H. Strihed, and B. Petersson, Ark. Fys. 39, 471 (1969).

[144]R. E. Watson, J. F. Herbst, and J. W. Wilkins, Phys. Rev. B 14, 18 (1976).

[145]Note that the gas-phase core-ionization energies in Table I, with the exception of Kr, differ from those used by Citrin and Hamann.[18] For Ne (Ref. 75) and Ar (Ref. 140) we use soft x-ray-emission data. The Xe value[52] is obtained from electron spectroscopy using monochromatized Al $K\alpha$ radiation. The Kr $3p_{3/2}$ value is probably the one which is impaired with the largest error. The main reason for this is not that it is obtained without monochromatization, but rather because of fairly strong configuration interaction effects which are due to an energy match between the $3p$ hole states and states of type $3\underline{d}^2nl$ (Ref. 52). In the core-level shift measurements the choice of the $3p_{3/2}$ level for Kr is therefore somewhat unfortunate.

[146]K. S. Kim and N. Winograd, Chem. Phys. Lett. 30, 91 (1975).

[147]W. D. Wilson and R. A. Johnson, in *Interatomic Potentials and Simulation of Lattice Defects*, edited by P. C. Gehlen, J. R. Beeler, Jr., and R. I. Jaffe (Plenum, New York, 1972), p. 375.

[148]For example, the study by Baer in Ref. 68 of solid (i.e., semimetallic) and liquid (i.e., metallic) bismuth shows that the $4f_{7/2}$ binding energy is practically identical for the two phases.

[149]B. Johansson and N. Mårtensson (unpublished).

[150]B. Johansson, J. Phys. F 4, L169 (1974).

[151]W. L. Jolly, in *Electron Spectroscopy*, edited by D. A. Shirley (North-Holland, Amsterdam, 1972), p. 690.

[152]N. Mårtensson and B. Johansson (unpublished).

[153]B. R. Judd, Phys. Rev. 125, 613 (1962).

[154]J. Reader and G. Epstein, J. Opt. Soc. Am. 63, 1153 (1973).

[155]H. Benschop, Y. N. Joshi, and Th. A. M. Vankleef, Can. J. Phys. 53, 700 (1975).

[156]B. Edlén, Phys. Scr. 17, 565 (1978).

[157]A. Bergström, Phys. Scr. 3, 157 (1971).

[158]P. Hellentin, Phys. Scr. 13, 155 (1976).

[159]J. Reader, G. L. Epstein, and J. O. Ekberg, J. Opt. Soc. Am. 62, 273 (1972).

[160]A. G. Shenstone, J. Res. Nat. Bur. Stand. 74A, 801 (1970).

[161]G. H. Newson, Astrophys. J. 166, 243 (1971); G. Mehlmann and J. M. Esteva, Astrophys. J. 188, 191 (1974).

[162]The averaging we have made is best illustrated by the example of potassium. First we note that the spin-orbit splitting is 2096 and 2162 cm^{-1} for the K I(p^5s^2) and K III(p^5) configurations, respectively. The average of these two values is taken to be the spin-orbit splitting of the p^5 configuration in K II(p^5s) when decoupled from the s electron. Then we calculate the average of the levels of the K II(p^5s) configuration [with individual weights of $(2J+1)$]; 162507.0 ($J=2$), 163237.0 ($J=1$), 165149.5 ($J=0$), and 166461.5 ($J=1$) (all in units of cm^{-1})[58]. This average level is then spin-orbit splitted by 2129 cm^{-1}. From this, the $P_{3/2}$ level of the decoupled K II(p^5s) configuration is found to be 20.233 eV above K II(p^6). Adding to this the first ionization potential 4.341 eV, we obtain the desired (decoupled) $p_{3/2}$ core-ionization energy 24.574 eV. The same type of procedure is applied to all the alkali and coin metals. It is only for cesium that the difference in the spin-orbit splitting between the first (p^5s^2) and third spectrum (p^5) is unreasonably large, the splittings being 9810 cm^{-1} and 13 884 cm^{-1}, respectively. Thus the derived (decoupled) experimental value for the $p_{3/2}$ ionization in cesium is somewhat uncertain.

[163]M. W. D. Mansfield and G. H. Newson, Proc. R. Soc. London 357, 77 (1977).

[164]Our inclusion of Cu in this connection does not mean

that we consider its d electrons as core electrons in the metallic phase. Instead, we use Cu as a test example of the present method for calculation of core-ionization energies. The same holds true later when we consider Ag and Au.

[165]The value for Zn is taken from Refs. 58 and 60. The value for Kr was obtained as described in Ref. 138. For Sr we have used the value in Ref. 69. The data for Cd were obtained from Ref. 71. Finally, for Xe Ref. 52 was consulted.

[166]The value for Yb was obtained from Ref. 59. For Hg Ref. 19 was used.

[167]The atomic calculations by Huang *et al.*[81] were used in the following way: first we compared the actually calculated values with the experimental ones for Zn, Kr, Sr, Cd and Xe.[164] The following deviations were found: Zn 2.92, Kr 1.77, Sr 1.17, Cd 0.88, and Xe 0.54 eV. These differences appear to behave rather smoothly. Assuming now that the deviations decrease uniformly within each interval, we derive correction energies for the intermediate elements.

[168]M. W. D. Mansfield and J. P. Connerade, Proc. R. Soc. London, Ser. A 344, 303 (1975). Additional lines were interpreted and revised ionization energies were given in a later publication. J. P. Connerade and M. W. D. Mansfield, Proc. R. Soc. London, Ser. A 348, 539 (1976).

[169]Essentially the same procedure as described in Ref. 166 was applied to the $4f_{7/2}$ binding energies. Here the deviation between the calculated[81] and experimental energies was 4.98 eV for Yb and 2.48 eV for Hg. For elements beyond Hg the deviations were linearly extrapolated.

[170]The approximation of using the same α for Rn, Th, and U is likely to be rather good. This is supported by cursory calculations for the outermost p level of related elements. The values in column 12 of Table III could thereby generally be reproduced to within 0.5 eV, using the appropriate α for the Ar $2p_{3/2}$ level.